Acknowledgments

Appendix A. Supplementary data

Supplementary data related to this article can be found online at http://dx.doi.org/10.1016/j.parkreldis.2012.06.019.

References

[1] Hutton M, Lendon CL, Rizzu P, Baker M, Froelich S, Houlden H, et al. Association of missense and 5'-splice-site mutations in tau with the inherited dementia FTDP-17. Nature 1998;393:702–5.

[2] Baker M, Mackenzie IR, Pickering-Brown SM, Gass J, Rademakers R, Lindholm C, et al. Mutations in progranulin cause tau-negative frontotemporal dementia linked to chromosome 17. Nature 2006;442:916–9.

[3] Cruts M, Gijselinck I, van der Zee J, Engelborghs S, Wils H, Pirici D, et al. Null mutations in progranulin cause ubiquitin-positive frontotemporal dementia linked to chromosome 17q21. Nature 2006;442:920–4.

[4] Dejesus-Hernandez M, Mackenzie IR, Boeve BF, Boxer AL, Baker M, Rutherford NJ, et al. Expanded GGGGCC hexanucleotide repeat in noncoding region of C9ORF72 causes chromosome 9p-linked FTD and ALS. Neuron 2011; 72:245–56.

[5] Renton AE, Majounie E, Waite A, Simon-Sanchez J, Rollinson S, Gibbs JR, et al. A hexanucleotide repeat expansion in C9ORF72 is the cause of chromosome 9p21-Linked ALS-FTD. Neuron 2011;72:257–68.

[6] Boeve BF, Hutton M. Refining frontotemporal dementia with parkinsonism linked to chromosome 17: introducing FTDP-17 (MAPT) and FTDP-17 (PGRN). Arch Neurol 2008;65:460–4.

[7] Murray ME, Dejesus-Hernandez M, Rutherford NJ, Baker M, Duara R, Graff-Radford NR, et al. Clinical and neuropathologic heterogeneity of c9FTD/ALS associated with hexanucleotide repeat expansion in C9ORF72. Acta Neuropathol 2011;122:673–90.

[8] Lindquist S, Duno M, Batbayli M, Puschmann A, Braendgaard H, Mardosiene S, et al. Corticobasal and ataxia syndromes widen the spectrum of C9ORF72 hexanucleotide expansion disease. Clin Genetics 2012 May 31 [Epub ahead of print].

[9] Neary D, Snowden JS, Gustafson L, Passant U, Stuss D, Black S, et al. Frontotemporal lobar degeneration: a consensus on clinical diagnostic criteria. Neurology 1998;51:1546–54.

[10] Mesulam MM. Slowly progressive aphasia without generalized dementia. Ann Neurol 1982;11:592–8.

[11] Litvan I, Agid Y, Calne D, Campbell G, Dubois B, Duvoisin RC, et al. Clinical research criteria for the diagnosis of progressive supranuclear palsy (Steele-Richardson-Olszewski syndrome): report of the NINDS-SPSP international workshop. Neurology 1996;47:1–9.

[12] Boeve BF, Lang AE, Litvan I. Corticobasal degeneration and its relationship to progressive supranuclear palsy and frontotemporal dementia. Ann Neurol 2003;54(Suppl. 5):S15–9.

[13] Baker M, Kwok JB, Kucera S, Crook R, Farrer M, Houlden H, et al. Localization of frontotemporal dementia with parkinsonism in an Australian kindred to chromosome 17q21-22. Ann Neurol 1997;42:794–8.

[14] Keyser RJ, Lombard D, Veikondis R, Carr J, Bardien S. Analysis of exon dosage using MLPA in South African Parkinson's disease patients. Neurogenetics 2010;11:305–12.

[15] Varani L, Hasegawa M, Spillantini MG, Smith MJ, Murrell JR, Ghetti B, et al. Structure of tau exon 10 splicing regulatory element RNA and destabilization by mutations of frontotemporal dementia and parkinsonism linked to chromosome 17. Proc Natl Acad Sci U S A 1999;96:8229–34.

[16] Kobayashi T, Ota S, Tanaka K, Ito Y, Hasegawa M, Umeda Y, et al. A novel L266V mutation of the tau gene causes frontotemporal dementia with a unique tau pathology. Ann Neurol 2003;53:133–7.

[17] Clark LN, Poorkaj P, Wszolek Z, Geschwind DH, Nasreddine ZS, Miller B, et al. Pathogenic implications of mutations in the tau gene in pallido-ponto-nigral degeneration and related neurodegenerative disorders linked to chromosome 17. Proc Natl Acad Sci U S A 1998;95:13103–7.

[18] Spillantini MG, Yoshida H, Rizzini C, Lantos PL, Khan N, Rossor MN, et al. A novel tau mutation (N296N) in familial dementia with swollen achromatic neurons and corticobasal inclusion bodies. Ann Neurol 2000;48:939–43.

[19] Ogaki K, Motoi Y, Li Y, Tomiyama H, Shimizu N, Takanashi M, et al. Visual grasping in frontotemporal dementia and parkinsonism linked to chromosome 17 (microtubule-associated with protein tau): a comparison of N-Iso-propyl-p-[(123)I]-iodoamphetamine brain perfusion single photon emission computed tomography analysis with progressive supranuclear palsy. Mov Disord 2011;26:561–3.

[20] Ghika J, Tennis M, Growdon J, Hoffman E, Johnson K. Environment-driven responses in progressive supranuclear palsy. J Neurol Sci 1995;130:104–11.

[21] Ogaki K, Li Y, Atsuta N, Tomiyama H, Funayama M, Watanabe H, et al. Analysis of C9orf72 repeat expansion in 563 Japanese patients with ALS. Neurobiol Aging 2012 June 21 [Epub ahead of print].

[22] Pierrot-Deseilligny C, Gautier JC, Loron P. Acquired ocular motor apraxia due to bilateral frontoparietal infarcts. Ann Neurol 1988;23:199–202.

[23] Leigh RJZD. In: The neurology of eye movements. 4 ed. New York: Oxford University Press; 2006. p. 512–21, 638–45.

[24] Rohrer JD, Paviour D, Vandrovcova J, Hodges J, de Silva R, Rossor MN. Novel L284R MAPT mutation in a family with an autosomal dominant progressive supranuclear palsy syndrome. Neurodegener Dis 2011;8:149–52.

[25] Williams DR, Pittman AM, Revesz T, Lees AJ, de Silva R. Genetic variation at the tau locus and clinical syndromes associated with progressive supranuclear palsy. Mov Disord 2007;22:895–7.

[26] Morris HR, Osaki Y, Holton J, Lees AJ, Wood NW, Revesz T, et al. Tau exon 10 + 16 mutation FTDP-17 presenting clinically as sporadic young onset PSP. Neurology 2003;61:102–4.

[27] Rossi G, Gasparoli E, Pasquali C, Di Fede G, Testa D, Albanese A, et al. Progressive supranuclear palsy and Parkinson's disease in a family with a new mutation in the tau gene. Ann Neurol 2004;55:448.

[28] Ros R, Thobois S, Streichenberger N, Kopp N, Sanchez MP, Perez M, et al. A new mutation of the tau gene, G303V, in early-onset familial progressive supranuclear palsy. Arch Neurol 2005;62:1444–50.

[29] Kim HJ, Jeon BS, Yun JY, Seong MW, Park SS, Lee JY. Screening for MAPT and PGRN mutations in Korean patients with PSP/CBS/FTD. Parkinsonism Relat Disord 2010;16:305–6.

[30] Mesulam MM. Primary progressive aphasia—a language-based dementia. N Engl J Med 2003;349:1535–42.

[31] Imai Y, Hasegawa K. The revised hasegawa's dementia scale (HDS-R) − evaluation of its usefulness as a screening test for dementia. J Hong Kong Coll Psychiatr 1994;4:20–4.

VPS35 Mutation in Japanese Patients with Typical Parkinson's Disease

Maya Ando, MD,[1] Manabu Funayama, PhD,[1,2*] Yuanzhe Li, MD, PhD,[2] Kenichi Kashihara, MD, PhD,[3] Yoshitake Murakami, MD,[4] Nobutaka Ishizu, MD,[5] Chizuko Toyoda, MD,[6] Katsuhiko Noguchi, MD,[7] Takashi Hashimoto, MD,[8] Naoki Nakano, MD,[9] Ryogen Sasaki, MD, PhD,[10] Yasumasa Kokubo, MD, PhD,[10] Shigeki Kuzuhara, MD, PhD,[11] Kotaro Ogaki, MD,[1] Chikara Yamashita, MD,[1] Hiroyo Yoshino, PhD,[2] Taku Hatano, MD, PhD,[1] Hiroyuki Tomiyama, MD, PhD,[1,12] and Nobutaka Hattori, MD, PhD[1,2,12*]

[1]Department of Neurology, Juntendo University School of Medicine, Tokyo, Japan
[2]Research Institute for Diseases of Old Age, Graduate School of Medicine, Juntendo University, Tokyo, Japan
[3]Department of Neurology, Okayama Kyokuto Hospital, Okayama, Japan
[4]Department of Neurology, Saiseikai Kurihashi Hospital, Saitama, Japan
[5]Department of Neurology, Saitama National Hospital, Saitama, Japan
[6]Department of Neurology, Jikei Daisan Hospital, Tokyo, Japan
[7]Department of Neurology, Kakio Kinen Hospital, Tokyo, Japan
[8]Hashimoto Clinic, Osaka, Japan
[9]Department of Neurosurgery, Kinki University Hospital, Osaka, Japan
[10]Department of Neurology, Mie University Graduate School of Medicine, Tsu, Mie, Japan
[11]Department of Medical Welfare, Faculty of Health Science, Suzuka University of Medical Science, Suzuka, Mie, Japan
[12]Department of Neuroscience for Neurodegenerative Disorders, Juntendo University School of Medicine, Tokyo, Japan

ABSTRACT: Vacuolar protein sorting 35 (VPS35) was recently reported to be a pathogenic gene for late-onset autosomal dominant Parkinson's disease (PD), using exome sequencing. To date, VPS35 mutations have been detected only in whites with PD. The aim of the present study was to determine the incidence and clinical features of Asian PD patients with VPS35 mutations. We screened 7 reported nonsynonymous missense variants of VPS35, including p.D620N, known as potentially disease-associated variants of PD, in 300 Japanese index patients with autosomal dominant PD and 433 patients with sporadic PD (SPD) by direct sequencing or high-resolution melting (HRM) analysis. In addition, we screened 579 controls for the p.D620N mutation by HRM analysis. The p.D620N mutation was detected in 3 patients with autosomal dominant PD (1.0%), in 1 patient with SPD (0.23%), and in no controls. None of the other reported variants of VPS35 were detected. Haplotype analysis suggested at least 3 independent founders for Japanese patients with p.D620N mutation. Patients with the VPS35 mutation showed typical tremor-predominant PD. We report Asian PD patients with the VPS35 mutation. Although VPS35 mutations are uncommon in PD, the frequency of such mutation is relatively higher in Japanese than reported in other populations. In VPS35, p.D620N substitution may be a mutational hot spot across different ethnic populations. Based on the clinical features, VPS35 should be analyzed in patients with PD, especially autosomal dominant PD or tremor-predominant PD. © 2012 Movement Disorder Society

Key Words: Parkinson's disease; VPS35; autosomal dominant; hotspot; mutation.

Parkinson's disease (PD) is a neurodegenerative disorder characterized by progressive motor disturbances manifested by tremor, rigidity, akinesia, and postural instability. Neuropathologically, PD is characterized by selective loss of dopaminergic neurons in the substantia nigra and the presence of cytosolic inclusions called Lewy bodies (LBs) in the remaining neurons. The pathogenesis of PD is multifactorial, including genetic–environmental interaction. PD is a common disease in the elderly, with an incidence of about 1%–2% in individuals older than 60 years.[1] Among PD patients, approximately 5%–10% have a positive family history of PD,[2] and among these, the Mendelian forms of PD can contribute to the elucidation of the molecular pathways that lead to the degeneration and death of dopaminergic neurons.

Mutations in the vacuolar protein sorting 35 (VPS35) gene have recently been identified in families with autosomal dominant late-onset PD (MIM 601501).[3,4] Patients with VPS35 mutations present with tremor-predominant dopa-responsive parkinsonism.[3,4] VPS35, a key component of the retromer cargo-recognition complex, is thought to associate with sorting cargos into the tubular endosomal network for retrieval to the trans-Golgi network.[5] Therefore, pathogenic mutations of VPS35 may cause disruption of the retrograde transport system and contribute to dopaminergic neuronal cell death in PD. One missense mutation has been reported to be pathogenic for PD.[3,4] Mutation of c.1858G>A (p.D620N) was identified in 3 Austrian families and 1 family each in Switzerland, the United States, Tunisia, and the United Kingdom, as well as 1 family and 1 patient with sporadic PD (SPD) among Yemenite Jews from Israel.[3,4,6] In addition, several variants, such as p.M57I, p.I241M, p.P316S, and p.R524W, have been reported in Europe and the United States as potentially pathogenic for PD.[3,4]

Although multipopulation screenings for VPS35 mutations were preformed in recent reports, there is still no report of PD patients with VPS35 mutations of Asian ancestry.[3,4,6–8] In the present study, we screened Japanese patients with autosomal-dominant PD (ADPD), Japanese patients with SPD, and control subjects for mutations of VPS35, with a special focus on 7 reported nonsynonymous variants that were found in patients with PD, including the p.D620N. Here, we report 3 families and 1 SPD patient with the p.D620N mutation in VPS35 and describe their clinical features.

Patients and Methods

Subjects

The study was approved by the ethics committee of Juntendo University, and all subjects gave written informed consent to participate in the genetic research. The study subjects were 308 Japanese patients (300 index patients) with ADPD (age at disease onset [AAO; mean ± SD], 51.1 ± 11.7 years; range, 8–83 years; female/male [F/M] ratio, 1.35) and 433 Japanese SPD patients (AAO, 47.2 ± 12.9 years; range, 5–88 years; F/M ratio, 1.09) selected from the gene bank of Juntendo University. Some of the selected subjects had been confirmed negative for SNCA, PARK2, PINK1, PARK7, LRRK2, and PLA2G6 mutations.[9–14] From the same gene bank, we also selected 579 healthy Japanese subjects without a family history of parkinsonism (age at sampling, 58.0 ± 9.3 years; range, 23–89 years; F/M ratio, 1.54). The criteria for the diagnosis of PD were adopted by the participating neurologists and were established based on the United Kingdom Parkinson's Disease Society Brain Bank.[15]

Genetic Analysis

Genomic DNA was extracted from peripheral blood using a standard protocol. Patients with ADPD and SPD were examined for the following 7 variants: p.M57I (exon 3), p.I241M (exon 7), p.P316S (exon 9), p.R524W (exon 13), p.D620N (exon 15), p.A737V (exon 16), and p.L774M (exon 17) of VPS35 (RefSeq accession number NM_018206.4). PCR direct sequencing was performed using a BigDye Terminator v1.1 Cycle Sequencing kit and 3130 Genetic Analyzer (Applied Biosystems, Foster City, CA) or 3730 DNA Analyzer (Applied Biosystems). In addition, SPD patients and control subjects were also genotyped for c.1858G>A (p.D620N) mutation by high-resolution melting (HRM) analysis using Light-Scanner and LCGreen plus (Idaho Technology, Salt Lake City, UT). HRM analysis was performed using a previously described protocol[16] and the following primers: forward, GAGGATGGTTGGTCCTTGAA; reverse, TGCCAATGATCAAGGTGATG. All exons of VPS35 were also analyzed in patients with the p.D620N mutation using the method described previously.[3]

Haplotype analysis of the VPS35 flanking region was performed using 3130 Genetic analyzer and Gene-Mapper software (Applied Biosystems, Foster City, CA). To adjust the size of PCR products, we also genotyped Centre d'Étude du Polymorphisme Humain (CEPH) control samples (1331-01 and 1331-02) for comparison of haplotypes with previously reported patients carrying the p.D620N mutation. The sequences of the PCR primers were reported previously.[3]

Results

Detection of p.D620N Mutation

We detected the heterozygous missense p.D620N mutation in 3 unrelated patients with ADPD and 1
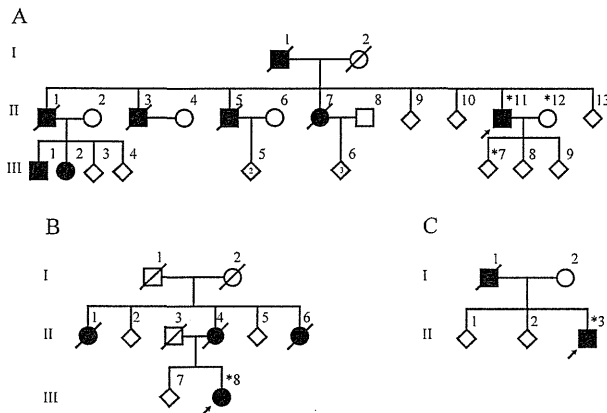
A

B C

FIG. 1. Pedigrees of families with the *VPS35* p.D620N mutation (open symbol, unaffected family member; closed symbol, affected member; arrow, proband; asterisk, individual analyzed for the p.D620N mutation and/or haplotype; forward slash through symbol, deceased individuals; square, male; circle, female; diamond, unspecified sex).

patient with SPD (Fig. 1). The p.D620N has been reported previously as a pathogenic mutation for familial PD.[3,4,6] This mutation was not found in 1158 control chromosomes. Patients carrying the p.D620N mutation did not have any other variants in all exons of *VPS35*. In our population, the incidence of the p.D620N mutation was 1.0% (3 of 300) in ADPD and 0.23% (1 of 433) in SPD. The remaining variants analyzed in this study were not identified in any patients.

Haplotype analysis demonstrated that the Japanese patients with the p.D620N mutation had different genotypes from those of white patients with the same mutation.[3] One disease allele was detected by analyzing patient AII-11 and his relatives. Patients AII-11 and BIII-8 in this study carried at least the same single allele of microsatellites in the flanking region of *VPS35* (Table 1). On the other hand, patients CII-3 and D had a different genotype of D16S3105, with a locus mapped very close to *VPS35*, compared with the disease allele of AII-11 (Table 1, boldface).

TABLE 1. Haplotype analysis of VPS35 p.D620N mutation carriers

	Patient ID			
Microsatellite	AII-11	BIII-8	CII-3	D
D16S401	170	166/170	166/172	166/170
D16S3068	143	141/145	145/147	145/145
D16S753	272	272/268	268/276	264/268
VPS35 p.D620N	A	A/G	A/G	A/G
Chr16_45.333M	294	294/298	294/300	294/304
D16S3105	191	191/189	189/193	187/187
Chr16_45.615M	147	147/147	147/145	147/145
Chr16_45.806M	246	246/238	246/244	246/244
Chr16_45.835M	237	237/237	237/237	237/237
Chr16_45.855M	212	212/210	210/210	210/216
D16S3044	195	195/195	195/197	197/197

Both alleles are shown when markers of phase could not be determined.

TABLE 2. Clinical features of patients with p.D620N mutation

	Patient ID			
	AII-11	BIII-8	CII-3	D
Age at disease onset (y)	62	55	34	42
Disease duration (y)	15	2	7	21
Resting tremor	+	+	+	+
Bradykinesia	+	+	+	+
Rigidity	+	+	+	+
Gait disturbance	+	−	−	+
Postural instability	+	−	−	+
Clinical response to levodopa	+	+	+	+
Wearing off	+	−	+	+
Asymmetry at onset	+	+	+	+
Orthostatic hypotension	+	−	−	−
Incontinence	+	−	−	−
Urinary urgency	−	−	−	−
Levodopa-induced dyskinesia	+	−	+	+
Sleep benefit	+	−	+	Unknown
Dystonia at onset	−	−	−	−
Hyperreflexia	−	−	−	−
Hallucination	−	−	−	−
Other psychosis	−	−	−	−
Dementia	+	−	−	−
Gaze palsy	−	−	−	−
Brain MRI	WNL	WNL	WNL	WNL
Cardiac MIBG scintigraphy	H/M ratio (E/L), 2.38/2.68; washout ratio, 4.15%[a]	Not performed	Not performed	Not performed

[a]MIBG scintigraphy was performed when AII-11 was 76 years old.
WNL, within normal limit; H/M ratio, heart-to-mediastinum ratio; (E/L), early/late stage.

Clinical Presentation

Table 2 summarizes the clinical features of the 4 *VPS35* mutation-positive patients. Patient AII-11 was a 77-year-old man who developed right upper limb rest tremor at age 62. At age 75, he underwent gastrostomy for progressive dysphagia, then developed cognitive dysfunction without hallucination. Single-photon emission computed tomography of cerebral blood flow showed no reduction in blood flow in the basal ganglia. His father and 4 of 8 siblings were diagnosed with PD (Fig. 1A) and presented levodopa-responsive typical parkinsonism: upper limb tremor and small-step gait. His nephew and niece were also diagnosed with PD, and the nephew developed parkinsonism in his early fifties. Patients BIII-8 and CII-3 both developed upper limb rest tremor at ages 34 and 55, respectively. The mother and aunts of patient BIII-8

and the father of patient CII-3 also developed PD (Fig. 1B, C). Patient D, who developed upper limb rest tremor at age 42, had no family history of PD. She underwent subthalamic nucleus deep brain stimulation (STN-DBS) at age 60 because of disabling motor fluctuation and dyskinesia refractory to pharmacological treatment. All affected patients were born to nonconsanguineous parents.

Discussion

VPS35 has been reported as the pathogenic gene for ADPD, and only 1 mutation, p.D620N, has been reported in several unrelated white families. To our knowledge, there have been no reports of Asian PD patients with VPS35 mutations.[3,8] Based on this background, we set out in this study to determine the incidence of VPS35 mutations in Japanese patients with PD. We detected the heterozygous p.D620N mutation of VPS35 in 3 ADPD families and 1 SPD patient with East Asian ancestry. On the other hand, we could not conclude the pathogenicity of 6 other variants that had been reported as potentially pathogenic for PD because none of the variants was detected in our patients with PD.

The frequency of the p.D620N mutation in Japanese patients was 1.0% in ADPD and 0.23% in SPD. Although the exact frequency among whites is undetermined, the frequency is relatively higher in Japanese patients compared with that reported in previous studies (0%–1.22%).[3,4,6,7,17] Moreover, the frequency in Japanese patients also differs greatly from those of other Asian populations such as Taiwanese patients and mainland Chinese patients (0%).[3,8] Although the mutation frequency was expected to be lower than that of other pathogenic genes for ADPD, such as multiplication of SNCA[9,18] and point mutation of LRRK2,[19–21] VPS35 may be one of the most important genes in Japanese PD. Because we screened for only 7 reported variants, we cannot determine the exact frequency of VPS35 mutations in ADPD; we would need to analyze all 17 exons of VPS35 in ADPD patients to screen for other variants and to assess the incidence of all disease-associated VPS35 mutations.[3,4] Furthermore, we would need to perform mutational analysis for SPD patients, in addition to ADPD, to identify Asian population-specific variants, such as LRRK2 p.G2385R, associated with susceptibility for PD.[19]

Based on haplotype analysis reported in previous studies, the substitution of VPS35 c.1858G>A (p.D620N) occurs from independent mutational events.[3] We were able to determine the chromosomal phase only in patient AII-11 (family A). The p.D620N mutation possibly shared a common founder between Japanese ADPD families A and B; however, it was inconclusive because the phase of patient BIII-8 was

undetermined. On the other hand, the same p.D620N mutation probably occurred independently in patient CII-3 (family C) and patient D. By genotyping of D16S3105, which is located approximately 1.5 kb centromeric of VPS35, there were at least 3 different haplotypes in Japanese because families A and C and patient D (SPD) did not have the same alleles for this microsatellite. To determine the chromosomal phase of families B and C, detailed genetic analyses of other family members are needed in future studies. These results suggest the existence of 3 or more founders in Japanese patients, in addition to the reported white patients with the p.D620N mutation or de novo mutations, indicating that the p.D620N mutation site is a mutational hot spot in VPS35 across different ethnic populations.

According to previous reports, the average AAO of patients with the VPS35 mutation was 50–60 years (50.6 ± 7.3 years),[3] with a distinctive feature of a slightly younger AAO compared with patients with idiopathic PD. In our study, the AAO was nonspecific with a wide range between 30–70 years. Because the family history of patient D was unknown, she was categorized as SPD. With regard to VPS35 mutation penetrance, it is incomplete from the results of a previous report.[3] Therefore, although the frequency is low, patients with p.D620N mutation could be found among SPD patients.

The clinical symptoms of our patients with VPS35 mutation closely resembled the idiopathic PD form, with tremor-dominant dopa-responsive parkinsonism. Psychiatric problems were inconspicuous; however, dementia may occur in patients with a long disease course, similar to patient AII-11, who had PD for 15 years. Our patients with VPS35 mutations had normal brain MRI and cardiac MIBG scintigraphy. There have been no definite pathological mutations of VPS35 in the spectrum of LB disorders. On the basis of these results, patients with VPS35 mutation could show comparatively benign disease course without widespread LBs pathology.[22,23]

VPS35 assembles into the retromer cargo-recognition complex that associates with the cytosolic face of the endosomes. The retromer mediates the retrograde transport of transmembrane cargo from the endosomes to the trans-Golgi network.[5] The p.D620N mutation of VPS35 might cause impairment of interaction with other components of the retromer complex and impaired retrograde trafficking of recycling proteins,[4] similar to α-synuclein and LRRK2, which are involved in vesicle trafficking.[24,25] Mutations in familial PD genes, including VPS35, may cause disruption of intracellular trafficking and lead to neurodegeneration. These findings suggest that impairment of intracellular trafficking systems is associated with the pathogenesis of PD. Although the association between the p.D620N mutation of VPS35 and PD remains unknown, further functional studies might shed light on the pathogenesis

of *VPS35* mutation and the effects of interaction with other known pathogenic gene products on PD.

In conclusion, we have reported Asian PD patients with the *VPS35* p.D620N mutation. The p.D620N substitution may be a mutational hot spot across different ethnic populations. The frequency of *VPS35* mutation was low in ADPD; however, it is relatively high in Japanese patients compared with that reported in other populations.[3,4,6–8] Based on the clinical features of patients with *VPS35* mutation, *VPS35* should be analyzed in patients with PD, especially ADPD or tremor-predominant PD. ▪

References

1. Lang AE, Lozano AM. Parkinson's disease. First of two parts. N Engl J Med 1998;339:1044–1053.

2. Lesage S, Brice A. Parkinson's disease: from monogenic forms to genetic susceptibility factors. Hum Mol Genet 2009;18:R48–R59.

3. Vilariño-Güell C, Wider C, Ross OA, et al. VPS35 mutations in Parkinson disease. Am J Hum Genet 2011;89:162–167.

4. Zimprich A, Benet-Pagès A, Struhal W, et al. A mutation in VPS35, encoding a subunit of the retromer complex, causes late-onset Parkinson disease. Am J Hum Genet 2011;89:168–175.

5. Bonifacino JS, Hurley JH. Retromer. Retromer. Curr Opin Cell Biol 2008;4:427–436.

6. Sheerin UM, Charlesworth G, Bras J, et al. Screening for VPS35 mutations in Parkinson's disease. Neurobiol Aging 2012;4:838.e1–e5.

7. Guella I, Soldà G, Cilia R, et al. The Asp620asn mutation in VPS35 is not a common cause of familial Parkinson's disease. Mov Disord 2012;27:800–801.

8. Zhang Y, Chen S, Xiao Q, et al. Vacuolar protein sorting 35 Asp620Asn mutation is rare in the ethnic Chinese population with Parkinson's disease. Parkinsonism Relat Disord 2012;18:638–640.

9. Nishioka K, Hayashi S, Farrer MJ, et al. Clinical heterogeneity of alpha-synuclein gene duplication in Parkinson's disease. Ann Neurol 2006;59:298–309.

10. Kitada T, Asakawa S, Hattori N, et al. Mutations in the parkin gene cause autosomal recessive juvenile parkinsonism. Nature 1998;392:605–608.

11. Kumazawa R, Tomiyama H, Li Y, et al. Mutation analysis of the PINK1 gene in 391 patients with Parkinson disease. Arch Neurol 2008;65:802–808.

12. Tomiyama H, Li Y, Yoshino H, et al. Mutation analysis for DJ-1 in sporadic and familial parkinsonism: screening strategy in parkinsonism. Neurosci Lett 2009;455:159–161.

13. Tomiyama H, Li Y, Funayama M, et al. Clinicogenetic study of mutations in LRRK2 exon 41 in Parkinson's disease patients from 18 countries. Mov Disord 2006;21:1102–1108.

14. Yoshino H, Tomiyama H, Tachibana N, et al. Phenotypic spectrum of patients with PLA2G6 mutation and PARK14-linked parkinsonism. Neurology 2010;75:1356–1361.

15. Hughes AJ, Daniel SE, Kilford L, Lees AJ. Accuracy of clinical diagnosis of idiopathic Parkinson's disease: a clinico-pathological study of 100 cases. J Neurol Neurosurg Psychiatry 1992;55:181–184.

16. Funayama M, Tomiyama H, Wu RM, et al. Rapid screening of ATP13A2 variant with high-resolution melting analysis. Mov Disord 2010;25:2434–2437.

17. Lesage S, Condroyer C, Klebe S et al. Identification of VPS35 mutations replicated in French families with Parkinson disease. Neurology 2012;78:1449–1450.

18. Ibáñez P, Lesage S, Janin S, et al. Alpha-synuclein gene rearrangements in dominantly inherited parkinsonism: frequency, phenotype, and mechanisms. Arch Neurol 2009;66:102–108.

19. Seki N, Takahashi Y, Tomiyama H, et al. Comprehensive mutational analysis of LRRK2 reveals variants supporting association with autosomal dominant Parkinson's disease. J Hum Genet 2011;56:671–675.

20. Di Fonzo A, Rohe C. F, Ferreira J, et al. A frequent LRRK2 gene mutation associated with autosomal dominant Parkinson's disease. Lancet 2005;365:412–415.

21. Gilks WP, Abou-Sleiman PM, Gandhi S, et al. A common LRRK2 mutation in idiopathic Parkinson's disease. Lancet 2005;365:415–416.

22. Orimo S, Amino T, Yokochi M, et al. Preserved cardiac sympathetic nerve accounts for normal cardiac uptake of MIBG in PARK2. Mov Disord 2005;10:1350–1353.

23. Verstraeten A, Wauters E, Crosiers D, et al. Contribution of VPS35 genetic variability to LBD in the Flanders-Belgian population. Neurobiol Aging 2012;33:e11–e13.

24. Caudle WM, Colebrooke RE, Emson PC, et al. Altered vesicular dopamine storage in Parkinson's disease: a premature demise. Trends Neurosci 2008;31:303–308.

25. Berwick DC, Harvey K. LRRK2 signaling pathways: the key to unlocking neurodegeneration? Trends Cell Biol 2011;21:257–265.

Contents lists available at SciVerse ScienceDirect

Parkinsonism and Related Disorders

journal homepage: www.elsevier.com/locate/parkreldis
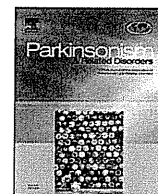
LRRK2 I2020T mutation is associated with tau pathology

Sachiko Ujiie [a,b], Taku Hatano [a,*], Shin-ichiro Kubo [a], Satoshi Imai [a,c], Shigeto Sato [a], Toshiki Uchihara [d], Saburo Yagishita [e], Kazuko Hasegawa [f], Hisayuki Kowa [b], Fumihiko Sakai [g], Nobutaka Hattori [a]

[a] Department of Neurology, Juntendo University, School of Medicine, 2-1-1 Hongo, Bunkyo-ku, Tokyo 113-8421, Japan
[b] Department of Neurology, Kitasato University, School of Medicine, 1-15-1 Kitasato, Minami-ku, Sagamihara, Kanagawa 252-0329, Japan
[c] Department of Toxicology, Hoshi University, School of Pharmacy and Pharmaceutical Sciences, 2-4-41 Ebara, Shinagawa-ku, Tokyo 142-8501, Japan
[d] Department of Neurology, Tokyo Metropolitan Institute for Neuroscience, 2-6 Musashidai, Fuchu, Tokyo 183-8526, Japan
[e] Department of Pathology, Kanagawa Rehabilitation Center, 516 Nanasawa, Atsugi, Kanagawa 243-0121, Japan
[f] Department of Neurology, National Hospital Organization Sagamihara National Hospital, 18-1 Sakuradai, Minami-ku, Sagamihara, Kanagawa 252-0315, Japan
[g] Saitama International Headache Center, Saitama Neuropsychiatric Institute, 6-11-1 Honmachihigashi, Saitama Chuo-ku, Saitama 338-0003, Japan

ARTICLE INFO

ABSTRACT

Mutations in the leucine-rich repeat kinase 2 (LRRK2) gene are the most common cause of autosomal-dominant familial Parkinson's disease (FPD). The variable pathological features of LRRK2-linked FPD include Lewy bodies, degeneration of anterior horn cells associated with axonal spheroids, neurofibrillary tangles (NFTs) and TAR DNA-binding protein of 43 kDa (TDP-43) positive inclusion bodies. Furthermore, abnormal hyperphosphorylation of microtubule associated protein tau, in part generated by catalysis of protein kinases, has been reported to be involved in progressive neurodegeneration in a number of diseases, including FPD. Thus, we examined six patients carrying the LRRK2 I2020T mutation, a pathogenic mutation associated with PARK8, and found abnormal tau phosphorylation depositions in the brainstem. Additionally, we found LRRK2 I2020T enhanced tau phosphorylation in cultured cells co-expressing LRRK2-I2020T and 3 or 4-repeated tau. This is the first report describing the relationship between hyperphosphorylation of tau and LRRK2 I2020T.

© 2012 Elsevier Ltd. All rights reserved.

1. Introduction

Parkinson's disease (PD) is a common neurodegenerative disease, characterized by rigidity, bradykinesia, resting tremor and postural instability. Mutations in leucine-rich repeat kinase 2 (LRRK2) have been identified as the causative gene for PARK8-linked PD [1,2]. LRRK2, also known as PARK8, is a large protein of 2527 amino acids, with a molecular weight of approximately 280 kDa. LRRK2 contains multiple protein domains, including a leucine-rich repeat (LRR) domain, a ROC domain, a COR domain, a MAPKKK domain and a WD40 domain [2,3]. Various intracellular functions of LRRK2 have been reported, with alterations in its kinase activities thought to be critical for neuronal degeneration [4–7]. Interestingly, the LRRK2 I2020T mutation is located within the kinase domain and is also associated with altered kinase activity [6,8,9]. However, molecular studies have not shown a robust association between neuronal cell death and altered LRRK2 kinase activity, and the pathogenic mechanism of the LRRK2 I2020T mutation remains unknown.

Patients with LRRK2 mutations show pleomorphic neuropathologies, which are not unique to PD and show overlap with other neurodegenerative diseases. These include nigral degeneration with or without Lewy bodies (LB) [2,10–14], also observed in diffuse LB disease [2,12,13], anterior horn cell degeneration associated with axonal spheroids, similar to amyotrophic lateral sclerosis [2], and neurofibrillary tangles (NFTs), also observed in progressive supranuclear palsy (PSP) [2,11,14,15] and Alzheimer's disease (AD) [2,12,13]. Notably, PD cases with G2019S [15], Y1699C [11] or I1371V [16] LRRK2 mutations, have shown varied tau pathology. Similarly, Li et al. reported that tau was hyperphosphorylated in brain tissues from LRRK2-R1441G overexpressing mice, compared with LRRK2 wild type (WT) mice [17]. In addition, G2019S overexpressing mice [18] and Drosophila [19], exhibited tau alterations including mislocalization and hyperphosphorylation. Therefore, we investigated the relationship between the LRRK2 I2020T mutation and tau phosphorylation. We examined brain tissue from the Sagamihara family, a Japanese kindred originally reported to be linked to the PARK8 locus [20], and found abnormally increased deposits of phosphorylated tau in the brainstem. Additionally, we showed that LRRK2 I2020T enhances tau phosphorylation in cultured cells co-expressing both LRRK2-I2020T and 3 or 4-repeated tau.

* Corresponding author. Tel.: +81 3 38133111; fax: +81 3 58000547.
E-mail address: thatano@juntendo.ac.jp (T. Hatano).

However, there was no direct interaction between mutant LRRK2 and tau proteins. Our results indicate that the presence of the pathological I2020T mutation causes hyperphosphorylation of tau and may participate in the pathogenesis of PD and other tau-associated neurodegenerative diseases. Our findings contribute to the understanding of PARK8 pathogenesis.

2. Material and methods

2.1. Subjects

We examined the brains of six patients who came to autopsy. The clinical findings of patients A-E have been reported previously [20,22,23]. In this report patient A represents case 3, B case 4,C case 5 D case 9 E case 10 from the previous report [23]. All patients showed a good response to levodopa developing motor complications in the later stages of their disease, consistent with idiopathic PD. None had marked autonomic or cognitive dysfunction.

Patient F was a 68-year-old female. At 51 years of age, she developed clumsiness in the legs and gait disturbance, and was diagnosed with PD. Treatment with levodopa resulted in a marked improvement of her symptoms. She developed "wearing-off" motor fluctuations at age 57. By 64 years, she had developed visual hallucinations; by age 65, she was unable to walk without assistance. At She died at age 68 of multiple organ failure caused by pneumonia. You have said this already above. This patient was genetically determined to have the I2020T amino acid substitution in LRRK2.

2.2. Immunohistochemistry

Autopsy was performed within 6 h after death in each case. Brain sections were fixed in formalin and representative areas were embedded in paraffin and sectioned. Brain sections were stained with hematoxylin-eosin (H&E) for histological examination. For immunohistochemistry, sections of all patients were deparaffinized and incubated with the following primary antibodies: rabbit polyclonal antibody against ubiquitin (Dako; 1:800), and mouse monoclonal antibodies against phosphorylated α-synuclein (#64; Wako; 1:10,000) and phosphorylation-dependent tau (AT8; Innogenetics, 1:10,000). Primary antibodies were incubated overnight at 4 °C and then visualized by the avidin-biotin-peroxidase complex method. In addition, brain sections were stained with three repeat (3R) or four repeat (4R) tau-specific antibodies (RD3; 1:3000 or RD4; 1:1000 respectively; Upstate) [24], after pretreatment with potassium permanganate and oxalic acid to eliminate non-specific staining [25].

2.3. Construct preparation

pRK5-FLAG-LRRK2-WT and LRRK2-I2020T mutant vectors were prepared as described previously [21]. Three or 4 repeat tau cDNA was amplified from human adult brain using reverse transcript PCR and cloned into Myc-pcDNA 3.1(–). The rabbit polyclonal anti-LRRK2 antibody with synthetic peptides at the C-terminal end (2510-2527 aa) of human LRRK2 was generated as described previously [21]. Monoclonal mouse anti-human PHF-tau antibodies (clone AT-180 and clone AT-270), and tau antibody (clone HT-7) were from Innogenetics. Secondary antibodies conjugated to horseradish peroxidase were from GE HealthCare Bio-Sciences.

2.4. Cell Culture and transfection

COS-1 cells were grown in Dulbecco's modified Eagle's medium (Sigma–Aldrich) supplemented with 10% fetal bovine serum (Sigma–Aldrich) and 1% penicillin/streptomycin (Invitrogen) under an atmosphere of 5% CO_2 at 37 °C. COS-1 cells were transiently transfected with LRRK2 and tau vectors using FuGENE HD Transfection Reagent (Roche Diagnostics) according to the manufacturer's protocol.

2.5. Immunoblotting

After 96 h, cells were lysed in lysis buffer containing 50 mM Tris–HCl (pH 7.4), 150 mM NaCl, 1% nonidet P-40, 0.25% DOC, 400 μM Na_3VO_4, 400 μM EDTA, 1 mM EGTA, 10 mM NaF, 10 mM sodium pyrophosphate and protease inhibitors (Complete Mini, EDTA-free; Roche Diagnostics). To detect LRRK2, the samples were resolved on 3–8% NuPAGE Tris-acetate polyacrylamide gels (Invitrogen) in 1 × NuPAGE Tris-Acetate SDS running buffer and transferred onto polyvinylidene fluoride (PVDF) membrane. The membranes were blocked for 1 h in PBS containing 0.05% Tween-20 (PBS-T) and 5% non-fat milk (BD Difco) and then incubated overnight at 4 °C with the primary antibody. The membranes were washed with PBS-T three times followed by incubation for 1 h at room temperature with horseradish peroxidase-conjugated anti-rabbit IgG (1:4000) and immunoreactivity assessed by chemiluminescence reaction using Western Lightning ECL (Perkin Elmer-Cetus). To detect tau, samples were resolved on 10% NuPAGE Bis-Tris polyacrylamide gels (Invitrogen) in 1 × NuPAGE MOPS SDS running buffer and transferred onto PVDF membrane. The membranes were blocked for 1 h in TBS containing 0.05% Tween-20 (TBS-T) and 5% non-fat milk (BD Difco) and then incubated overnight at 4 °C with the primary antibody. The membranes were washed with TBS-T buffer three times followed by incubation for 1 h at room temperature with horseradish peroxidase-conjugated anti-mouse IgG (1:2000). The remaining steps were as described above. Blots were quantified using Image J software analysis.

2.6. Immunoprecipitation

Cell lysates were centrifuged at 15,000× g for 20 min at 4 °C and the resulting supernatant fluid was incubated with Anti-FLAG M2 Agarose (Sigma–Aldrich) overnight at 4 °C. The resin was separated by centrifugation, washed three times with lysis buffer and then boiled in Laemmli sample buffer. Finally, each sample was analyzed by SDS-PAGE followed by immunoblotting.

2.7. Statistical analysis

Three group comparisons were analyzed by UNI-ANOVA followed by Turkey's multiple comparison tests (SPSS). All values were expressed as mean ± SEM. A P value less than 5% denoted a statistically significant difference among the groups.

3. Results

3.1. Variable tau pathology in PD associated with LRRK2 I2020T mutation

A previous pathological study of LRRK2 I2020T patients reported an apparent loss of nigral neurons without LBs, with the exception of onecase with LBs. However extensive immunohistochemical analysis of phosphorylated tau was not performed.

The pathological features of patients A-E have been described previously [23]. The additional new patient (patient F) shared neuropathological features with patients A-E, as follows [23]. Macroscopic examination revealed marked discoloration of the substantia nigra (SN) (Fig. 1a), with a well preserved locus coeruleus (LC) (Fig. 1b). This region-specific contrast in neuropathology was confirmed following microscopic examination, with marked neuronal loss, gliosis and extraneuronal melanin present in SN (Fig. 1c), in contrast to well preserved neurons with minimal gliosis in LC (Fig. 1d). Of note, the dorsal motor nucleus of the vagus nerve (DVN) appeared predominantly normal. In addition, we observed Marinesco bodies, ubiquitin-positive intranuclear inclusions, in the surviving neuromelanin-containing SN neurons (Fig. 1e).

Characteristics of the tau-positive lesions are summarized in **Table 1**. Patient B and E had tau-positive lesions restricted to the brainstem, namely SN, LC and the trochlear nucleus (Fig. 2a). In patients C and D, abnormal phosphorylated tau depositions were observed not only in the brainstem but also in the hippocampus and amygdala. Senile plaques were not found in any regions. In patients A and F, there were no tau-positive lesions. Immunohistochemistry with isoform-specific antibodies, determined that the tau-positive lesions contained both 3R and 4R tau (Fig. 2b, c). Overall, these results show that the I2020T mutation causes autosomal-dominant PD with a pleomorphic pathology, as observed with other LRRK2 mutations.

3.2. LRRK2 is associated with hyperphosphorylation of tau

Based on our pathological findings in LRRK2 I2020T patients, we hypothesized that mutant LRRK2 may be involved in hyperphosphorylation of tau. To determine the effect of LRRK2 I2020T on tau phosphorylation, we co-transfected COS-1 cells with LRRK2-WT or I2020T and 4R tau. Levels of phosphorylated tau and total tau were assessed by western blotting using antibodies, which recognize tau phosphorylation, AT-180 at Thr231 and AT-270 at Thr181 (Fig. 3c, d). Neither LRRK2-WT nor I2020T changed expression levels of total tau protein (Fig. 3c, d). However, significantly increased levels of phosphorylated 4R tau were detected in cells with overexpressed LRRK2-I2020T, but not WT (AT-180: 100.0 ± 1.2% [mean ± SEM] with WT vs. 118.5 ± 1.5% with I2020T, $p < 0.001$; AT-
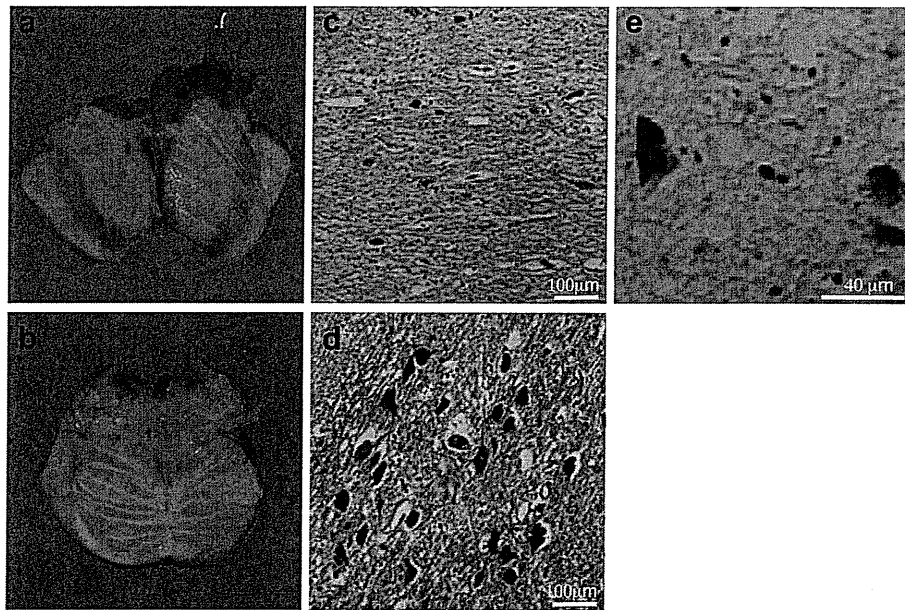
Fig. 1. Neuropathology of patient F, a LRRK2 I2020T carrier from the original Japanese Sagamihara family. Marked discoloration of the substantia nigra (SN, a) and relative preservation of locus coeruleus (LC, b). Marked neuronal loss with gliosis in the SN (c, H&E) is in contrast with preserved neurons in LC (d, H&E). Marinesco bodies are abundant in the SN (e, ubiquitin immunostain). Bars: c, d:100 µm; e: 40 µm.

270: $93.7 \pm 4.0\%$ with WT vs. $113.8 \pm 5.3\%$ with I2020T, $p < 0.001$; Fig. 3c, d). Next, we determined if I2020T affects expression levels of phosphorylated 3R tau. LRRK2-I2020T induced a significant, albeit modest, increase in the level of phosphorylated 3R tau protein compared with WT (AT-180: $94.9 \pm 2.4\%$ with WT vs. $100.5 \pm 6.5\%$ with I2020T, n.s.; AT-270: $93.5 \pm 1.2\%$ with WT vs. $104.1 \pm 2.5\%$ with I2020T, $p < 0.01$; Fig. 3a, b). To investigate further the interaction between LRRK2 and tau, we performed immunoprecipitation experiments. There was no evidence of a direct interaction between either LRRK2-WT or I2020T mutant with 4R tau (Fig. 3e).

4. Discussion

Tau pathology has been identified in the brains of PD patients with *LRRK2* mutations, with reports of various forms of tau depositions of, for example PSP-like or AD-like distribution and pattern of age related changes [26,27]. In this study, we identified tau pathology in four patients with *LRRK2 I2020T* mutation; an

increased amount of phosphorylated tau was associated with LRRK2 I2020T mutation compared to wild type in cultured cell models. In addition, we found that affected members of the Sagamihara family display a homogeneous pattern of neuronal loss, namely degeneration of the SN with relative preservation of LC and DVN. This is in sharp contrast to idiopathic PD, where involvement of LC and DVN is observed. We also identified Marinesco bodies in our patients. The presence of Marinesco bodies has been described in other *LRRK2*-linked PD patients with R1441C [2] and G2019S mutations [14]. Thus, mutant LRRK2 may possibly affect dopaminergic neurons by accelerating the formation of Marinesco bodies.

In contrast to the homogeneity of neuronal degeneration that we observed, deposits of α-synuclein were confirmed only in patient E, and tau-positive deposits in the brainstem nuclei also varied? among the subjects. In previous reported pathological findings of *LRRK2*-linked PD, the presence of LBs and tau deposits did not overlap, even in the same family, which is in agreement with our observations in the Sagamihara family. Cookson et al. reported that although clinical features of *LRRK2*-linked PD were similar to sporadic PD, the pathological findings varied, confounding the correlation between etiology and disease expression [29]. Similarly, all examined members of the Sagamihara family showed typical PD features irrespective of pathological deposits. In addition, we did not find a direct correlation between tau deposits and clinical symptoms. Tau-positive deposits were seen in the

Table 1
Summary of tau pathology in LRRK2 I2020T carriers from the Sagamihara family

	Patient A	Patient B	Patient C	Patient D	Patient E	Patient F
Hippocampus	−	−	+	+	−	−
Meynert	−	−	−	−	+	−
Amygdala	NA	−	−	++	NA	NA
IV	−	+++	++	−	NA	NA
LC	−	+	++	+	+	−
Central gray matter	−	−	++	−	−	−
SN	−	−	+	−	+	−
Braak stage	<1	<1	2	3	<1	<1

The severity and distribution of NFT pathology was estimated using Braak staging (Braak and Braak 1991) (− none; + mild; ++ moderate; +++ severe; n/a not applicable). Tau pathology was observed in 4 out of 6 patients. Two individuals (patient B and E) had tau-positive lesions restricted to the brainstem, with another two individuals (patient C and D), showing tau-positive lesions in the hippocampus as well as the brainstem. The remaining two patients (patient A and F) did not show tau-positive lesions in any brain regions. IV; trochlear nucleus, LC; locus coeruleus, SN; substantia nigra.
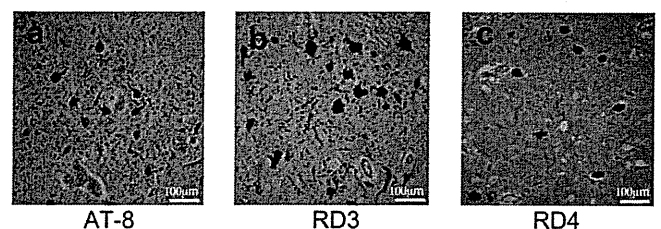

AT-8   RD3   RD4

Fig. 2. Tau pathology in patient B, a LRRK2 I2020T carrier. Representative immunohistochemical analysis of tau in the trochlear nerve nucleus from Patient B. Sections are labeled with AT8 (a), RD3 (b) and RD4 (c). Bars: c, d:100 µm; e: 40 µm.
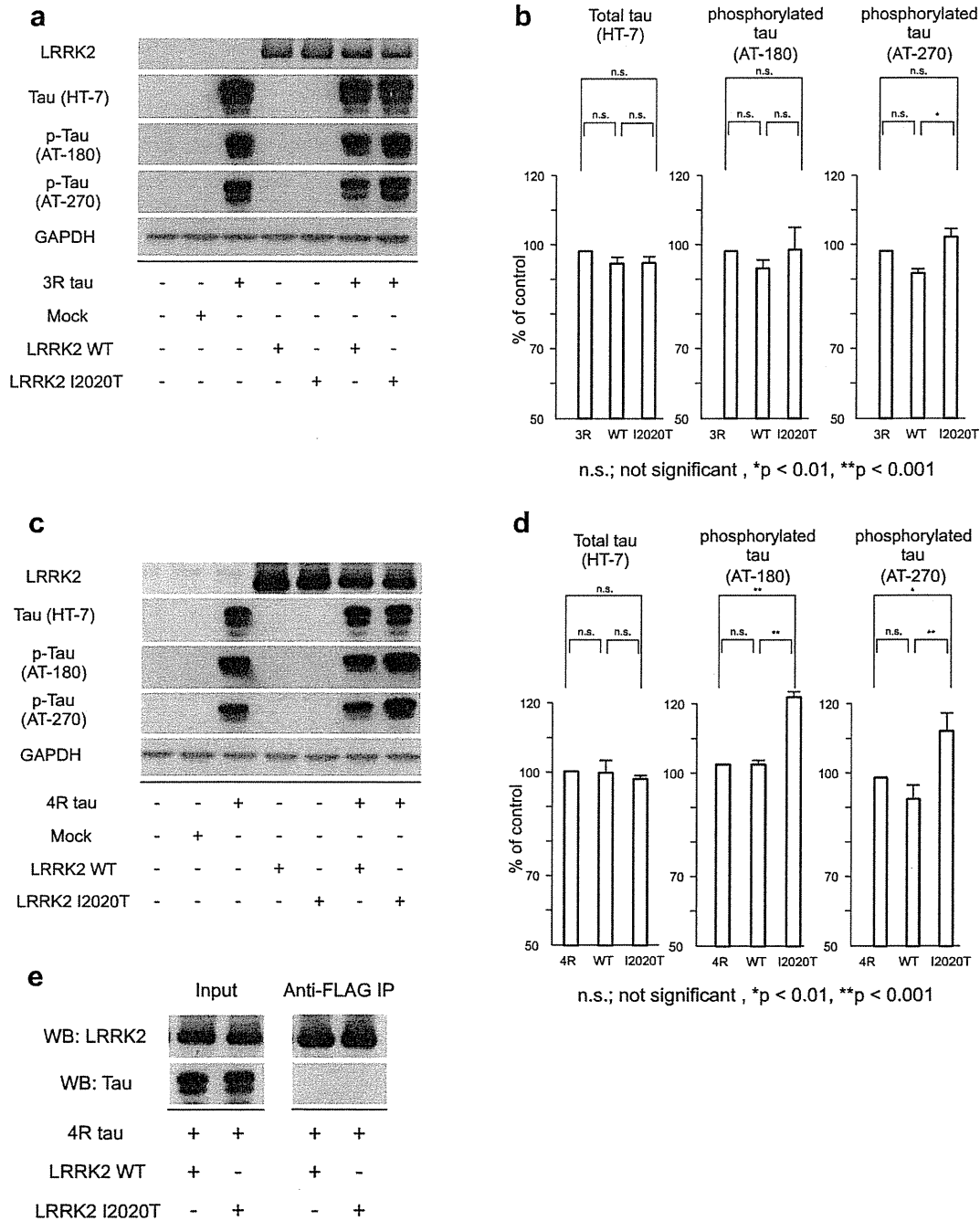
Fig. 3. LRRK2-I2020T induces increasing levels of phosphorylated tau compared with LRRK2-WT or mock transfected cells. (a, b) Lysate prepared from COS-1 cells co-expressing 3R tau and LRRK2-WT or I2020T, were subjected to anti-tau (HT-7) or anti-phosphorylated tau (AT-180 and AT-270) immunoblotting. LRRK2-I2020T increased expression levels of phosphorylated tau compared to LRRK2-WT, albeit modestly. (HT-7; 96.3 ± 1.8% with WT vs. 96.5 ± 1.9% with I2020T [mean ± SEM]; n.s., AT-180; 94.9 ± 2.4% with WT vs. 100.5 ± 6.5% with I2020T; n.s., AT-270; 93.5 ± 1.2% with WT vs. 104.1 ± 2.5% with I2020T; $p < 0.01$) (c, d). Lysate prepared from COS-1 cells co-expressing 4R tau and LRRK2-WT or I2020T, were subjected to anti-tau (HT-7) or anti-phosphorylated tau (AT-180 and AT-270) immunoblotting. LRRK2-I2020T significantly increased expression levels of phosphorylated tau compared to LRRK2-WT. (HT-7; 99.7 ± 3.5% with WT vs. 97.8 ± 1.1% with I2020T; n.s. AT-180; 100.0 ± 1.2% with WT vs. 118.5 ± 1.5% with I2020T; $p < 0.001$, AT-270; 93.7 ± 4.0% with WT vs. 113.8 ± 5.3% with I2020T; $p < 0.001$). (e) Lysate prepared from COS-1 cells transfected with Myc-4 repeats tau and FLAG-LRRK2-WT or FLAG-LRRK2-I2020T, were subjected to immunoprecipitation with anti-FLAG antibody followed by anti-tau (HT-7) immunoblotting. In the left panel, cell lysates were used to detect the expression of LRRK2 and tau. In the right panel, FLAG-LRRK2 was immunoprecipitated using FLAG antibody. Upper lanes show LRRK2 detected with anti-LRRK2 antibody. Lower lanes show that no bands were obtained with anti-HT-7 antibody. As a result, LRRK2 does not directly interact with 4R tau.

nucleus of the trochlear nerve in patients B and C, neither exhibited ophthalmoparesis. Consistent with these findings, Vitte et al. reported that LRRK2 protein is present throughout the human brain, with intense immunoreactivity in the neurons of several midbrain nuclei, including the nucleus of the trochlear nerve [28].

We then demonstrated the association between LRRK2 and tau hyperphosphorylation by using cultured cell models. Compared to LRRK2-WT or mock transfected, overexpression of LRRK2-I2020T in cultured cells resulted in increased levels of phosphorylated tau proteins. Furthermore, this increase in phosphorylated tau was

823

associated with upregulation of both 3R and 4R tau isoforms. These findings could provide support for abnormal hyperphosphorylated tau deposition in the pathological findings of patients with *LRRK2 I2020T* mutation.

Based on neuropathological findings and cultured cell models, we hypothesized that LRRK2 is able to enhance tau phosphorylation. Our immunoprecipitation studies showed no evidence of a direct interaction between either LRRK2-WT or I2020T mutant with tau, indicating that tau phosphorylation by LRRK2-I2020T involves the association of an intermediate, genetic, or environmental factor. Smith et al. also reported that LRRK2 failed to bind tau protein [30]. Furthermore, LRRK2 mutations have been reported to be associated with tau hyperphosphorylation without direct interaction in animal models. Li et al. reported that tau is hyperphosphorylated in brain tissues from LRRK2-R1441G overexpressing mice compared with LRRK2-WT mice [17]. Mice and drosophila overexpressing *LRRK2*-G2019S also exhibited tau alterations, including mislocalization and increased tau phosphorylation [18,19]. Therefore, we believe that LRRK2 mutations can be involved in the tau phosphorylation pathway.

How LRRK2 can participate in the tau phosphorylation pathway remains unclear. In addition, we failed to find that these abnormal tau deposits have any apparent spatial correlation with our observed region-specific neuronal degeneration in the Sagamihara family. Therefore, future work will need to evaluate the association between neurodegeneration and the tau hyperphosphorylation due to *LRRK2 I2020T* mutation.

Conflicts of interest

None declared.

Acknowledgements

References

[1] Paisan-Ruiz C, Jain S, Evans EW, Gilks WP, Simon J, van der Brug M, et al. Cloning of the gene containing mutations that cause PARK8-linked Parkinson's disease. Neuron 2004;44:595–600.

[2] Zimprich A, Biskup S, Leitner P, Lichtner P, Farrer M, Lincoln S, et al. Mutations in LRRK2 cause autosomal-dominant parkinsonism with pleomorphic pathology. Neuron 2004;44:601–7.

[3] Mata IF, Wedemeyer WJ, Farrer MJ, Taylor JP, Gallo KA. LRRK2 in Parkinson's disease: protein domains and functional insights. Trends Neurosci 2006;29: 286–93.

[4] Greggio E, Jain S, Kingsbury A, Bandopadhyay R, Lewis P, Kaganovich A, et al. Kinase activity is required for the toxic effects of mutant LRRK2/dardarin. Neurobiol Dis 2006;23:329–41.

[5] West AB, Moore DJ, Biskup S, Bugayenko A, Smith WW, Ross CA, et al. Parkinson's disease-associated mutations in leucine-rich repeat kinase 2 augment kinase activity. Proc Natl Acad Sci U S A 2005;102:16842–7.

[6] West AB, Moore DJ, Choi C, Andrabi SA, Li X, Dikeman D, et al. Parkinson's disease-associated mutations in LRRK2 link enhanced GTP-binding and kinase activities to neuronal toxicity. Hum Mol Genet 2007;16:223–32.

[7] Smith WW, Pei Z, Jiang H, Dawson VL, Dawson TM, Ross CA. Kinase activity of mutant LRRK2 mediates neuronal toxicity. Nat Neurosci 2006;9:1231–3.

[8] Gloeckner CJ, Kinkl N, Schumacher A, Braun RJ, O'Neill E, Meitinger T, et al. The Parkinson disease causing LRRK2 mutation I2020T is associated with increased kinase activity. Hum Mol Genet 2006;15:223–32.

[9] Imai Y, Gehrke S, Wang HQ, Takahashi R, Hasegawa K, Oota E, et al. Phosphorylation of 4E-BP by LRRK2 affects the maintenance of dopaminergic neurons in Drosophila. EMBO J 2008;27:2432–43.

[10] Gilks WP, Abou-Sleiman PM, Gandhi S, Jain S, Singleton A, Lees AJ, et al. A common LRRK2 mutation in idiopathic Parkinson's disease. Lancet 2005; 365:415–6.

[11] Khan NL, Jain S, Lynch JM, Pavese N, Abou-Sleiman P, Holton JL, et al. Mutations in the gene LRRK2 encoding dardarin (PARK8) cause familial Parkinson's disease: clinical, pathological, olfactory and functional imaging and genetic data. Brain 2005;128:2786–96.

[12] Ross OA, Toft M, Whittle AJ, Johnson JL, Papapetropoulos S, Mash DC, et al. Lrrk2 and Lewy body disease. Ann Neurol 2006;59:388–93.

[13] Giasson BI, Covy JP, Bonini NM, Hurtig HI, Farrer MJ, Trojanowski JQ, et al. Biochemical and pathological characterization of Lrrk2. Ann Neurol 2006;59: 315–22.

[14] Gaig C, Marti MJ, Ezquerra M, Rey MJ, Cardozo A, Tolosa E. G2019S LRRK2 mutation causing Parkinson's disease without Lewy bodies. J Neurol Neurosurg Psychiatry 2007;78:626–8.

[15] Rajput A, Dickson DW, Robinson CA, Ross OA, Dachsel JC, Lincoln SJ, et al. Parkinsonism, Lrrk2 G2019S, and tau neuropathology. Neurology 2006;67: 1506–8.

[16] Giordana MT, D'Agostino C, Albani G, Mauro A, Di Fonzo A, Antonini A, et al. Neuropathology of Parkinson's disease associated with the LRRK2 Ile1371Val mutation. Mov Disord 2007;22:275–8.

[17] Li Y, Liu W, Oo TF, Wang L, Tang Y, Jackson-Lewis V, et al. Mutant LRRK2(R1441G) BAC transgenic mice recapitulate cardinal features of Parkinson's disease. Nat Neurosci 2009;12:826–8.

[18] Melrose HL, Dachsel JC, Behrouz B, Lincoln SJ, Yue M, Hinkle KM, et al. Impaired dopaminergic neurotransmission and microtubule-associated protein tau alterations in human LRRK2 transgenic mice. Neurobiol Dis 2010;40:503–17.

[19] Lin CH, Tsai PI, Wu RM, Chien CT. LRRK2 G2019S mutation induces dendrite degeneration through mislocalization and phosphorylation of tau by recruiting autoactivated GSK3beta. J Neurosci 2010;30:13138–49.

[20] Funayama M, Hasegawa K, Kowa H, Saito M, Tsuji S, Obata F. A new locus for Parkinson's disease (PARK8) maps to chromosome 12p11.2-q13.1. Ann Neurol 2002;51:296–301.

[21] Hatano T, Kubo SI, Imai S, Maeda M, Ishikawa K, Mizuno Y, et al. Leucine-rich repeat kinase 2 associates with lipid rafts. Hum Mol Genet 2007;16:678–90.

[22] Funayama M, Hasegawa K, Ohta E, Kawashima N, Komiyama M, Kowa H, et al. An LRRK2 mutation as a cause for the parkinsonism in the original PARK8 family. Ann Neurol 2005;57:918–21.

[23] Hasegawa K, Stoessl AJ, Yokoyama T, Kowa H, Wszolek ZK, Yagishita S. Familial parkinsonism: study of original Sagamihara PARK8 (I2020T) kindred with variable clinicopathologic outcomes. Parkinsonism Relat Disord 2009;15: 300–6.

[24] de Silva R, Lashley T, Gibb G, Hanger D, Hope A, Reid A, et al. Pathological inclusion bodies in tauopathies contain distinct complements of tau with three or four microtubule-binding repeat domains as demonstrated by new specific monoclonal antibodies. Neuropathol Appl Neurobiol 2003;29: 288–302.

[25] Uchihara T, Nakamura A, Shibuya K, Yagishita S. Specific Detection of pathological three-repeat tau after pretreatment with potassium permanganate and oxalic acid in PSP/CBD brains. Brain Pathol 2011;21:180–8.

[26] Gaig C, Ezquerra M, Marti MJ, Valldeoriola F, Munoz E, Llado A, et al. Screening for the LRRK2 G2019S and codon-1441 mutations in a pathological series of parkinsonian syndromes and frontotemporal lobar degeneration. J Neurol Sci 2008;270:94–8.

[27] Taymans JM, Cookson MR. Mechanisms in dominant parkinsonism: the toxic triangle of LRRK2, alpha-synuclein, and tau. Bioessays 2010;32:227–35.

[28] Vitte J, Traver S, Maues De Paula A, Lesage S, Rovelli G, Corti O, et al. Leucine-Rich repeat kinase 2 is associated with the Endoplasmic Reticulum in dopaminergic neurons and Accumulates in the core of Lewy bodies in Parkinson disease. J Neuropathol Exp Neurol 2010;69:959–72.

[29] Cookson MR, Hardy J, Lewis PA. Genetic neuropathology of Parkinson's disease. Int J Clin Exp Pathol 2008;1:217–31.

[30] Smith WW, Pei Z, Jiang H, Moore DJ, Liang Y, West AB, et al. Leucine-rich repeat kinase 2 (LRRK2) interacts with parkin, and mutant LRRK2 induces neuronal degeneration. Proc Natl Acad Sci U S A 2005;102:18676–81.
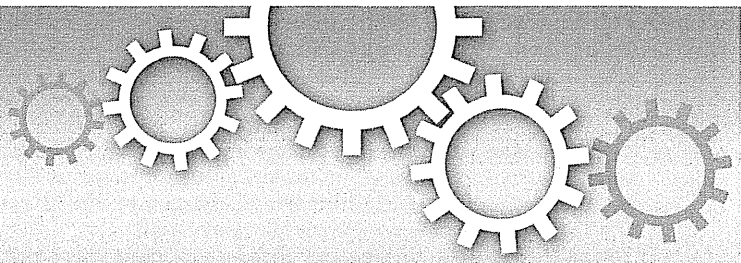
SCIENTIFIC REPORTS

PINK1-mediated phosphorylation of the Parkin ubiquitin-like domain primes mitochondrial translocation of Parkin and regulates mitophagy

Kahori Shiba-Fukushima[1], Yuzuru Imai[2], Shigeharu Yoshida[3], Yasushi Ishihama[3], Tomoko Kanao[4], Shigeto Sato[1] & Nobutaka Hattori[1,2,4,5]

[1]Department of Neurology, Juntendo University Graduate School of Medicine, Tokyo 113-8421, Japan, [2]Department of Neuroscience for Neurodegenerative Disorders, Juntendo University Graduate School of Medicine, Tokyo 113-8421, Japan, [3]Department of Molecular and Cellular BioAnalysis, Graduate School of Pharmaceutical Sciences, Kyoto University, Kyoto 606-8501, Japan, [4]Research Institute for Diseases of Old Age, Juntendo University Graduate School of Medicine, Tokyo 113-8421, Japan, [5]CREST (Core Research for Evolutionary Science and Technology), JST, Saitama 332-0012, Japan.

Parkinson's disease genes *PINK1* and *parkin* encode kinase and ubiquitin ligase, respectively. The gene products PINK1 and Parkin are implicated in mitochondrial autophagy, or mitophagy. Upon the loss of mitochondrial membrane potential ($\Delta\Psi$m), cytosolic Parkin is recruited to the mitochondria by PINK1 through an uncharacterised mechanism – an initial step triggering sequential events in mitophagy. This study reports that Ser65 in the ubiquitin-like domain (Ubl) of Parkin is phosphorylated in a PINK1-dependent manner upon depolarisation of $\Delta\Psi$m. The introduction of mutations at Ser65 suggests that phosphorylation of Ser65 is required not only for the efficient translocation of Parkin, but also for the degradation of mitochondrial proteins in mitophagy. Phosphorylation analysis of Parkin pathogenic mutants also suggests Ser65 phosphorylation is not sufficient for Parkin translocation. Our study partly uncovers the molecular mechanism underlying the PINK1-dependent mitochondrial translocation and activation of Parkin as an initial step of mitophagy.

M utations of the *PINK1* gene cause selective degeneration of the midbrain dopaminergic neurons in autosomal recessive juvenile Parkinson's disease (PD)[1]. The *PINK1* gene encodes a serine/threonine kinase with a predicted mitochondrial target sequence and a putative transmembrane domain at the N-terminus[2-5]. Loss of the *PINK1* gene in *Drosophila* results in the degeneration of mitochondria in cells with high energy demands, such as muscle and sperm cells, which is suppressed by the introduction of the *parkin* gene, another gene responsible for autosomal recessive juvenile PD[6-8]. The gene product Parkin encodes a RING-finger type ubiquitin ligase (E3) with a Ubl domain at the N-terminus[9-12].

A series of cell biological studies have provided strong evidence that there are important roles for PINK1 and Parkin in regulating mitochondrial homeostasis. PINK1 is constitutively proteolysed by the mitochondrial rhomboid protease, PARL, at the mitochondrial membrane of healthy mitochondria, resulting in processed forms of PINK1[13-16]. The processed PINK1 is rapidly degraded by the proteasome[2,17]. The reduction of $\Delta\Psi$m leads to the accumulation and activation of PINK1 in the mitochondria[17-19] through a currently unresolved mechanism[20]. The accumulation of PINK1 recruits Parkin from the cytosol to the mitochondria with decreased membrane potential, which stimulates Parkin E3 activity, promoting mitochondrial degradation via an autophagic event known as mitophagy[17,21-24]. The recruitment of cytosolic Parkin to the mitochondria upon disruption of $\Delta\Psi$m is believed to be the first step of mitophagy for the removal of damaged mitochondria. This recruitment is required for the kinase activity of PINK1[17,21-25]. Although two separate studies have proposed that Parkin is directly phosphorylated by PINK1[26,27], others have failed to detect Parkin phosphorylation by PINK1[21], suggesting that the kinase activity of PINK1 itself is relatively low. One reason biochemical analysis has been unable to obtain direct evidence is that recombinant human PINK1 purified from mammalian cultured cells or bacteria easily loses kinase activity, while insect PINK1 has significant autophosphorylation activity[28,29].

Very recently, Kondapalli, C. *et al.* reported that PINK1 directly phosphorylates Parkin at Ser65 in the Ubl domain[18]. However, the extent and consequences of Parkin phosphorylation by PINK1 in mitochondrial regulation are still not fully understood.

To address this issue, we attempted to independently monitor and compare the phosphorylation status of Parkin in wild-type and *PINK1*-deficient cells, thereby excluding the possibility of phosphorylations by uncharacterised kinases other than PINK1[30]. Here, we also report that Parkin is demonstrably phosphorylated at Ser65 in a PINK1-dependent manner. Furthermore, we show that this phosphorylation event is implicated in the regulation of mitochondrial translocation of Parkin and the subsequent degradation of mitochondrial surface proteins during mitophagy.

Results

Parkin is phosphorylated upon depolarisation in ΔΨm. We used [^{32}P] orthophosphate to metabolically label mouse embryonic fibroblasts (MEFs) derived from *PINK1* deficient mice, in which HA-tagged Parkin together with FLAG-tagged wild-type or kinase-dead forms (triple mutant with K219A, D362A and D384A) of PINK1 were virally introduced (hereafter referred to as "PINK1-FLAG WT" or "KD/HA-Parkin/*PINK1$^{-/-}$*" MEFs) and then induced Parkin-mediated mitophagy via treatment with the protonophore carbonyl cyanide *m*-chlorophenyl hydrazone (CCCP). As shown in Figure 1a, Parkin was specifically phosphorylated in CCCP-treated PINK1-FLAG WT/HA-Parkin/*PINK1$^{-/-}$* MEFs, but not in PINK1-FLAG KD/HA-Parkin/*PINK1$^{-/-}$* MEFs. Phos-tag Western blotting, in which phosphorylated proteins appear as slower migrating bands[28], revealed that Parkin was phosphorylated within 10 min following CCCP treatment (Fig. 1b). Phosphorylation of Parkin reached its maximum level approximately 40 min after CCCP treatment and was sustained at least until 6 hr (Supplementary Fig. S1). Under these conditions, slower migrating bands of PINK1 also appeared, which very likely reflects the autophosphorylation of PINK1 when activated (Fig. 1b)[18]. The suppression of PINK1 accumulation by RNA interference suggested thatΔΨm depolarisation-dependent activation of PINK1 along with PINK1 accumulation is a key element for Parkin phosphorylation (Fig. 1c). Every PINK1 deletion and pathogenic mutant we tested failed to stimulate Parkin phosphorylation effectively, strongly suggesting that intact PINK1 is required for this action (Fig. 1d and e). Importantly, human fibroblasts from a patient with *PINK1*-linked parkinsonism also lacked the activity to phosphorylate Parkin (Fig. 1f). The phosphorylated Parkin disappeared within 30 min during the recovery of ΔΨm depolarisation by the removal of CCCP from the culture medium (Fig. 1g). Further analysis using phosphatase and proteasome inhibitors suggested that phosphorylated Parkin is at least partly degraded by proteasomal activity in the mitochondria (Supplementary Fig. S2).

Phosphorylation of Ser65 in the Parkin Ubl domain primes the mitochondrial translocation of Parkin. To determine which residue(s) of Parkin are phosphorylated, we immunopurified HA-tagged Parkin from PINK1-FLAG WT or KD/HA-Parkin/*PINK1$^{-/-}$* MEFs treated with or without CCCP and performed mass spectrometric analysis for phospho-peptides (Supplementary Fig. S3). Although Phos-tag Western blotting of Parkin mainly detected a single band shift, which represents a single phospho-modification, the mass spectrometric analysis identified Ser9 or Ser10 and Ser65, Ser101 and Ser198 as phosphorylated residues of Parkin. Among these residues, only Ser65 phosphorylation increased (33-fold) in CCCP-treated PINK1-FLAG WT/HA-Parkin/*PINK1$^{-/-}$* MEFs (Supplementary Fig. S3). Phos-tag Western blotting with mutant forms of Parkin, in which the identified phospho-serine residues are replaced with alanine, revealed that the band shift represents Ser65 phosphorylation (Fig. 2a). An *in vitro* kinase assay with recombinant insect PINK1, which has marked kinase activity[28], strongly suggested that

PINK1 directly phosphorylates Parkin at Ser65 (Supplementary Fig. S4). The Ser65 residue lies in the Ubl domain and is highly conserved from human to *Drosophila* (Fig. 2b). We next examined whether phosphorylation of Ser65 is required for Parkin-mediated mitophagy. GFP-tagged Parkin WT, which was localised both in the cytoplasm and in the nuclei of mock (DMSO)-treated cells (0 hr, Fig. 2c and d), was translocated to the mitochondria and induced the perinuclear aggregation of mitochondria 2 hr after CCCP treatment, as previously reported (2 hr, Fig. 2c and d)[17,23]. Replacement of Ser65 with alanine (S65A) did not affect the subcellular localisation of Parkin in mock-treated cells when compared with that of GFP-Parkin WT (0 hr, Fig. 2c and d). However, GFP-Parkin S65A almost completely inhibited the mitochondrial translocation of Parkin and the perinuclear rearrangement of mitochondria 0.5 hr after CCCP treatment (0.5 hr, Fig. 2c and d) and showed delayed translocation in 2 hr (2 hr, Fig. 2c and d). The expression of a putative phosphomimetic Parkin S65E also showed a subcellular localisation similar to that of GFP-Parkin WT in both DMSO- and CCCP-treated cells (Fig. 2c). However, GFP-Parkin S65E exhibited a mild translocation defect, suggesting that S65E does not fully mimic the phosphorylated Ser65 (Fig. 2d).

Parkin Ser65 phosphorylation is not sufficient for mitochondrial translocation upon depolarisation of ΔΨm. As PINK1-mediated Ser65 phosphorylation appeared to be required for efficient translocation of Parkin, we next examined whether well-characterised pathogenic Parkin mutants were subjected to phosphorylation upon CCCP treatment. In this experiment, we used three kinds of Parkin mutants based on the previous and current studies (Supplementary Fig. S5)[17,22,23]. The first group, V15M, P37L, R42P and A46P, had intact or weakly impaired mitochondrial translocation activity. The second group, T415N and G430D, had mildly impaired translocation activity. The third group, K161N, K221N and T240R, almost completely lacked translocation activity (Fig. 3a). Surprisingly, all of the mutants possessed comparable phosphorylation efficiencies to those of WT (Fig. 3b). This result suggests that Ser65 phosphorylation is not sufficient for the mitochondrial translocation of Parkin.

Biochemical fractionation of endogenous Parkin from SH-SY5Y cells detected only the phosphorylated form of Parkin in the mitochondrial fraction upon CCCP treatment (Fig. 3c), which strongly suggests that phosphorylation of Parkin is required for mitochondrial translocation. There was a slight difference in the gel mobility of phosphorylated Parkin between the cytosolic and the mitochondrial fractions and between CCCP-treated periods of time. These differences very likely reflect differences in the complexity of the contents of each fraction rather than in the phosphorylation status of Parkin because a single shifted band appears in the mixed fractions (Mito + Cyto in Fig. 3c; CCCP 30 min + 60 min in Supplementary Fig. S6).

Effect of Parkin Ser65 phosphorylation on the autophagic reaction. We next examined whether Ser65 phosphorylation is required for the subsequent autophagic reaction, in which various ubiquitin-proteasome- and autophagy-related proteins are involved, including the 26S proteasome, p97/VCP, p62/SQSTM1, LC3, ATG5 and ATG7[22,23,31-35]. Parkin has been reported to be involved in the ubiquitin-proteasome-dependent degradation of a variety of mitochondrial outer membrane proteins, including Mitofusin1 (Mfn1)[32], Mfn2[32], Miro1[36,37], Miro2[37], VDAC1[22] and Tom20[31]. Degradation of Mfn1, VDAC1 and Tom20 at the mitochondrial outer membrane was observed in PINK1 WT/GFP-Parkin/*PINK1$^{-/-}$* MEFs 1 to 4 hr after CCCP treatment (Fig. 4a). While GFP-Parkin harbouring S65A or S65E mutations was also capable of inducing Mfn1, VDAC1 and Tom20 degradation, the efficiency was impaired, especially in Mfn1 and VDAC1 (Fig. 4a). Long-term time course analysis revealed that in cells expressing Parkin with S65A or S65E mutations, Mfn1 and VDAC1 cannot be degraded effectively, and the mitochondrial outer membrane was likely more intact as indicated by the sustained
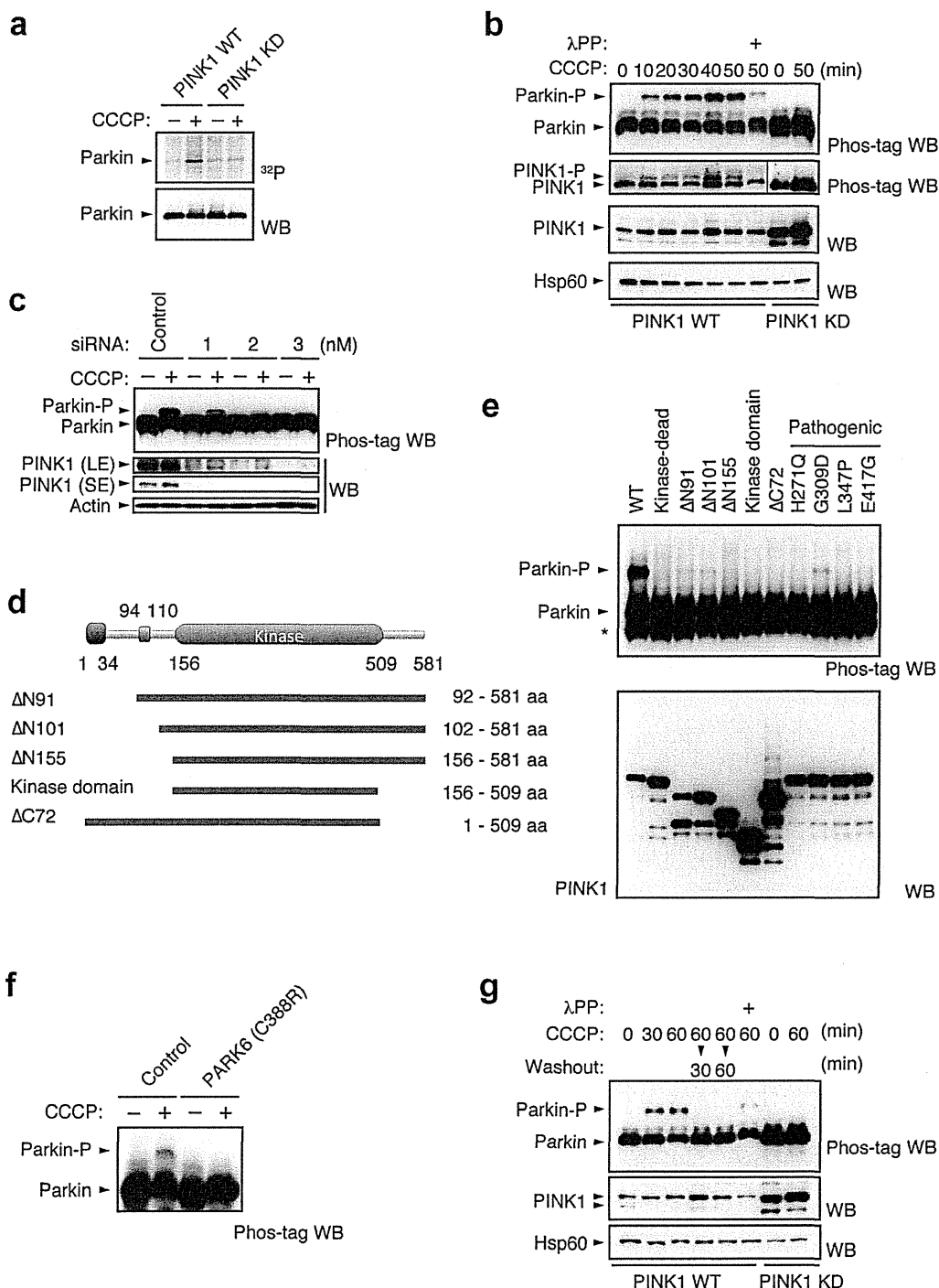
Figure 1 | PINK1-dependent phosphorylation of Parkin *in vivo*. (a) PINK1-FLAG WT or KD/HA-Parkin/*PINK1*^{−/−} MEFs were labelled with [³²P] orthophosphate and treated with 30 µM CCCP for 1.5 hr. Phosphorylated Parkin was detected by autoradiography (³²P). Immunoprecipitated HA-Parkin was detected by Western blotting (WB) with anti-Parkin. (b) PINK1-FLAG WT or KD/HA-Parkin/*PINK1*^{−/−} MEFs were treated with or without 30 µM CCCP for the indicated periods of time. Cell lysate was subsequently separated on a Phos-tag gel, followed by WB with anti-PINK1 or anti-Parkin antibodies (Phos-tag WB). Phosphorylated bands of Parkin and PINK1 were confirmed by their disappearance with lambda protein phosphatase (λPP) treatment. Mitochondrial Hsp60 was used as a loading control. (c) Suppression of endogenous PINK1 expression inhibits Parkin phosphorylation. HeLa cells stably expressing non-tagged Parkin were treated with the indicated concentrations of stealth siRNA duplex against PINK1 (Invitrogen) with or without 10 µM CCCP for 1 hr. Long- (LE) and short-exposure (SE) blot signals for PINK1 were shown. Actin was used as a loading control. (d) Truncated PINK1 mutants used in this study. Putative mitochondria-targeting sequence, 1–34 aa; transmembrane domain, 94–110 aa; kinase domain, 156–509 aa. (e) Full-length PINK1 is required for Parkin phosphorylation. *PINK1*^{−/−} MEFs stably expressing non-tagged Parkin were transfected with various PINK1 constructs with C-terminal FLAG-tags. PINK1 expression was confirmed with anti-FLAG-HRP. (f) Human fibroblasts from a normal control and a *PARK6* case with a homozygous C388R mutation[44] were transfected with Parkin and were treated with or without 30 µM CCCP for 1 hr. (g) Cells treated with CCCP up to 60 min as in (b) were further incubated with fresh culture medium without CCCP for the indicated periods of time (Washout).
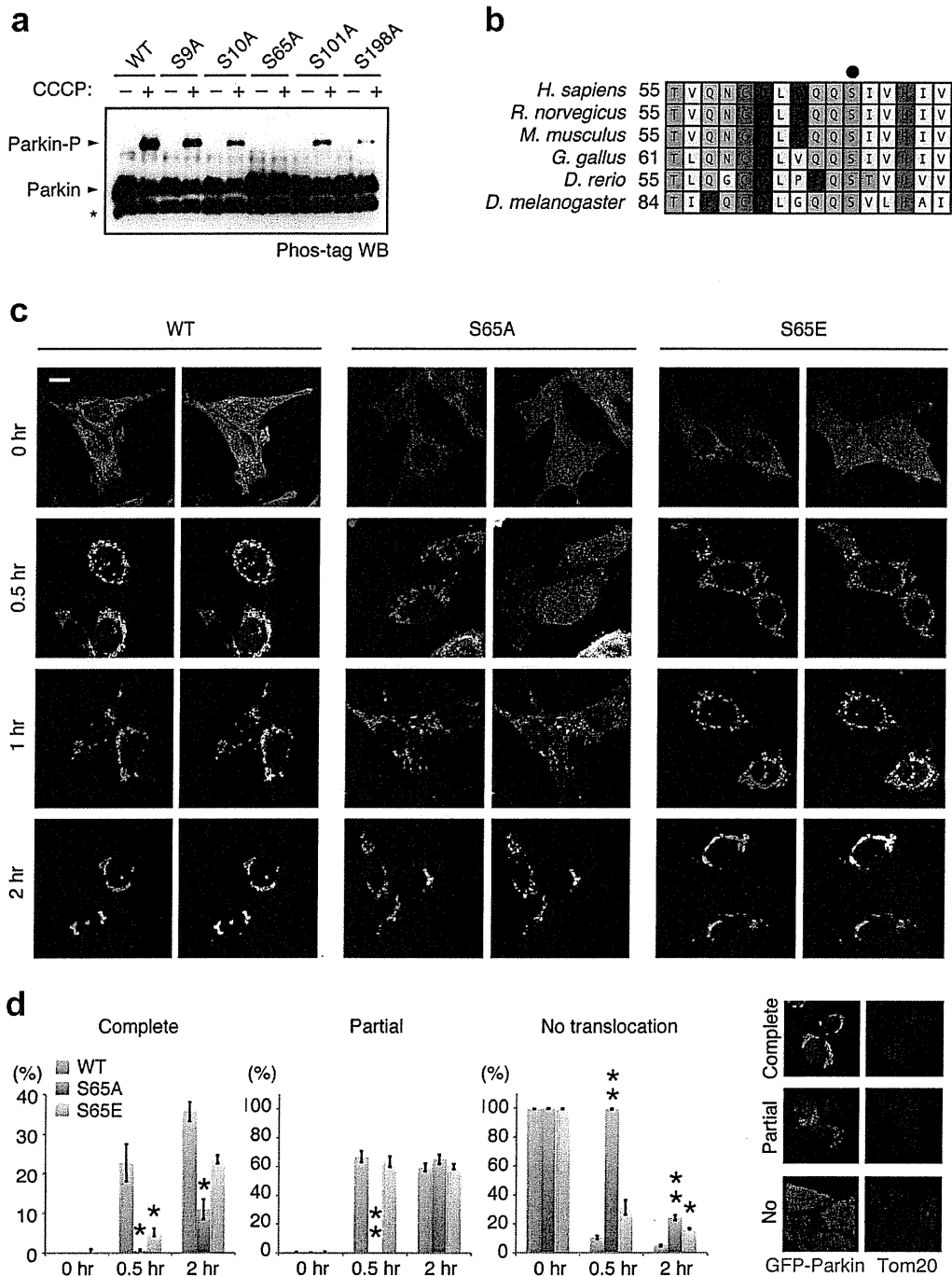
Figure 2 | Ser65 in the Ubl domain of Parkin is phosphorylated upon depolarisation of ΔΨm. (a) Phos-tag Western blotting detected phosphorylation of Ser65. HeLa cells were transiently transfected with Parkin WT and a series of alanine mutants for the candidate phospho-residues followed by treatment with or without 20 μM CCCP for 1 hr. Cell lysates were analysed by Phos-tag Western blotting. An asterisk indicates degraded Parkin. (b) Alignment of the amino acid sequences surrounding Ser65 (marked by a black dot) from a variety of animal species. The numbers on the left correspond to the residue numbers of Parkin proteins. (c) Introduction of the S65A mutation delayed Parkin translocation to the depolarised mitochondria in PINK1 WT/GFP-Parkin/$PINK1^{-/-}$ MEFs. Cells retrovirally introduced with GFP-Parkin WT or its phospho-mutants (S65A and S65E) were treated with or without 30 μM CCCP for the indicated periods of time. GFP-Parkin and mitochondria were visualised with anti-GFP (green) and anti-Tom20 (red), respectively. Parkin signals are also shown as monochrome images. Scale bar = 10 μm. (d) Mitochondrial translocation efficiency of Parkin mutants. PINK1 WT/$PINK1^{-/-}$ MEFs stably expressing GFP-Parkin WT, S65A or S65E were treated as in (c). Cells expressing GFP-Parkin perfectly overlapped (Complete, examples are shown on the right), partially overlapped (Partial) or non-overlapped (No) with the Tom20 signal were counted. The data represent means ± SE from three experiments (n = 99–143 cells in each). ** $p < 0.01$, * $p < 0.05$ vs. WT at each time point.
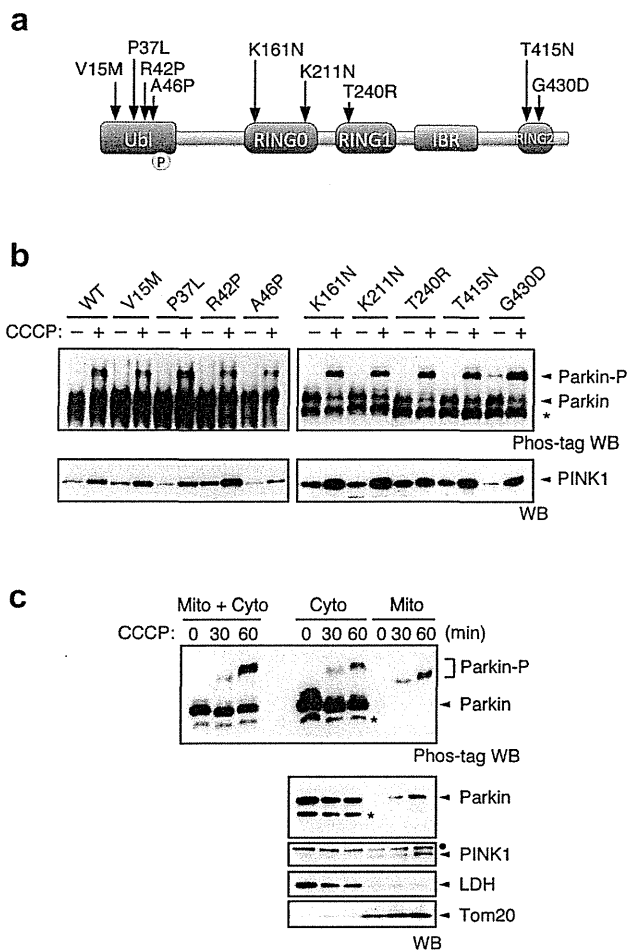
a

b

c

Figure 3 | Pathogenic mutants of Parkin are subjected to Ser65 phosphorylation. (a) Diagram of Parkin protein illustrating the pathogenic mutants used in this study. The Ser65 residue in the Ubl domain is shown as a yellow circle. RING, Ring-finger motif; IBR, in-between-Ring fingers domain. (b) Phos-tag Western blotting for Parkin and Western blotting for PINK1 were performed using Parkin WT and a series of pathogenic mutants as shown in Figure 2a. (c) Endogenous Parkin was also phosphorylated in SH-SY5Y cells after CCCP treatment. Post-nuclear cell lysates from SH-SY5Y cells treated with or without 10 μM CCCP for 30 and 60 min were fractionated into mitochondria-rich (Mito) and cytosolic (Cyto) fractions. These two fractions and their combination (Mito + Cyto) were subjected to Phos-tag or normal Western blotting analyses. Endogenous PINK1 was fractionated in the Mito fraction, as previously reported[45]. Lactate dehydrogenase (LDH) and Tom20 were used as cytosolic and mitochondrial marker proteins, respectively. Asterisks: putative cleaved Parkin; dots: non-specific bands.

accumulation of PINK1 (Fig. 4b). The impaired degradation cannot be explained simply by the delayed translocation of Parkin mutants because both mutants completed the mitochondrial translocation by the 6 hr time-point (data not shown and see Fig. 4c). In contrast, the profiles of Parkin expression and autoubiquitination in Parkin S65A- or S65E-expressing cells were comparable with those of WT (Fig. 4b). We also examined whether Ser65 mutations affect the accumulation of proteasome (Fig. 4c) and p62 (Supplementary Fig. S7) at the mitochondria during mitophagy via the immunostaining of the proteasome subunit alpha type 7 (α7) and p62. However, there was no evidence that Ser65 mutations inhibit or delay the recruitment of proteasome and p62 to the mitochondria. Finally, we tested whether the Parkin Ubl domain itself is indispensable for the mitochondrial

translocation and the substrate degradation (Supplementary Fig. S8). Interestingly, Parkin mutant lacking the Ubl domain (ΔUbl) showed a mild delay in the mitochondrial translocation, slowed the mitochondrial reorganization to the perinuclear region (Supplementary Fig. S8b and c) and impaired the degradation of mitochondrial outer membrane proteins (Supplementary Fig. S8d). These results suggest that proper regulation of the Parkin Ubl domain through the Ser65 phosphorylation is required not only for efficient translocation to mitochondria as an initial step of mitophagy, but also for the degradation of mitochondrial outer membrane proteins during mitophagy through an as yet unknown mechanism.

Discussion

A series of *Drosophila* genetic and cell biological studies have clearly demonstrated that PINK1 is required for Parkin-mediated mitochondrial maintenance. The mitophagy of damaged mitochondria is a well-characterised event in which PINK1 and Parkin are involved. However, how PINK1 regulates Parkin is largely unclear. This study has shown that Ser65 in the Ubl domain of endogenous Parkin is phosphorylated in an activated PINK1-dependent manner. In addition to mitochondrial accumulation of PINK1, ΔΨm depolarisation-dependent PINK1 autophosphorylation has been reported to be an important element for PINK1 activation and Parkin recruitment[19,29]. Consistent with these observations, our investigation of PINK1 siRNA suggests that a lower level of PINK1 is able to phosphorylate Parkin after ΔΨm depolarisation (Fig. 1c, compare lanes 1 and 4). Our domain analysis of PINK1 demonstrates that intact PINK1 is required for CCCP-dependent Parkin phosphorylation, and the lack of phosphorylation in fibroblasts from a *PARK6* patient implies relevance to the pathogenesis of PD.

The biological significance of this phosphorylation event is suggested by the fact that replacement of Ser65 with alanine or glutamic acid impairs the mitochondrial translocation of Parkin and/or the subsequent mitophagy process. Our observation that maximal phosphorylation of Parkin occurs within 1 hr of CCCP treatment supports the idea that Ser65 phosphorylation is required for the early step of Parkin translocation. In contrast, PINK1 accumulation appears to last at least 6 hr (Fig. 4c and Supplementary Fig. S1b). The difference in time course between PINK1 accumulation and Parkin phosphorylation could be explained by the observation that phosphorylated Parkin is degraded by proteasomal activity. The biochemical evidence that only the phosphorylated form of endogenous Parkin is present in the mitochondrial fraction also implies that Parkin phosphorylation is an essential event for its mitochondrial translocation and subsequent activation (Fig. 3c and Supplementary Fig. S6). Overexpression of PINK1 and Parkin itself leads to mitochondrial translocation of Parkin independently of ΔΨm depolarization, which suggests that excessive amounts of PINK1 and Parkin do not faithfully reflect endogenous reactions. Our study using *PINK1^{-/-}* MEFs stably co-expressing PINK1 and GFP-Parkin might also be saddled with such a problem. We believe that the endogenous observation in which phosphorylated Parkin is accumulated in mitochondria is a more reliable proposal as a molecular model. The delay of exogenous GFP-Parkin S65A in the mitochondrial translocation would indicate that modification of Ser65 is important for Parkin translocation at least. At the same time, another important finding is that pathogenic mutants that lose their translocation activity are also phosphorylated (Fig. 3b), raising the possibility that phosphorylation of Parkin at Ser65 is insufficient for translocation. Thus, Ser65 phosphorylation likely leads to other events in mitochondrial translocation, such as the association or dissociation of protein(s) involved in the mitochondrial translocation of Parkin or the modification of Parkin itself for activation at a different site(s).

Both the S65A and S65E Parkin mutants cannot undergo efficient mitophagy, as indicated by the incomplete degradation of
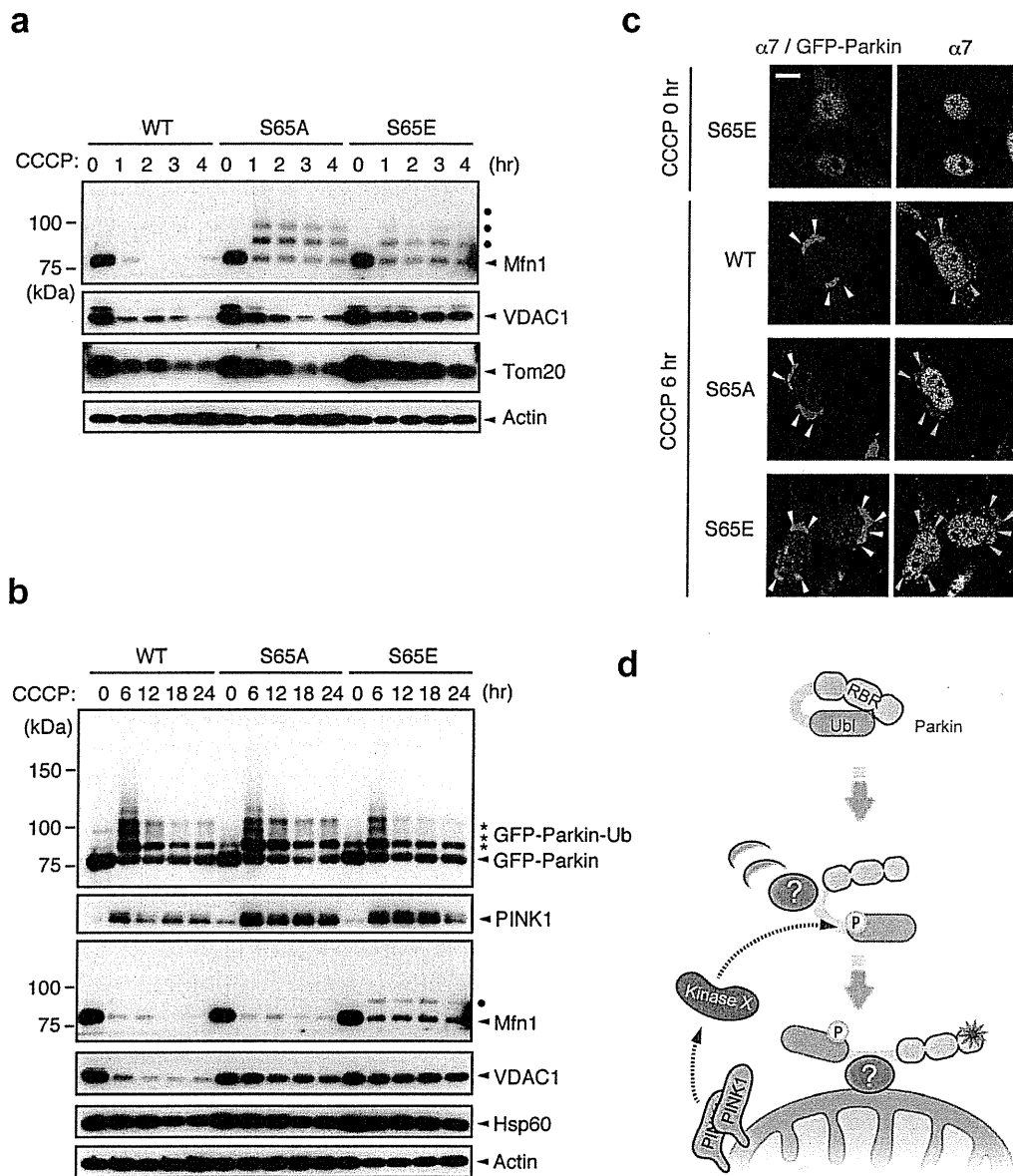
Figure 4 | Ser65 phosphorylation affects the subsequent autophagy reaction. (a) CCCP-dependent degradation of mitochondrial outer membrane proteins in PINK1 WT/*PINK1*−/− MEFs expressing WT or mutant forms of GFP-Parkin. Mfn1, VDAC1 and Tom20 were used as markers of mitochondrial outer membrane proteins. Actin: a loading control. Dots: ubiquitinated Mfn1. (b) Long-term time-course analysis of CCCP-dependent mitochondrial protein degradation. The degradation of outer membrane proteins was impaired in cells expressing GFP-Parkin S65A or S65E mutations. Hsp60 was used as a marker of mitochondrial matrix proteins. (c) S65A and S65E mutations do not affect proteasome recruitment to the mitochondria during mitophagy. PINK1 WT/*PINK1*−/− MEFs expressing WT or mutant forms of GFP-Parkin (green) were treated with 30 μM CCCP for 3 or 6 hr. Cells were stained with anti-proteasome subunit alpha type 7 (α7, red). α7-immunoreactivity was enriched in the nuclei of all three cell genotypes under normal conditions, as displayed in the representative image of S65E (CCCP 0 hr), and overlapped with the aggregated mitochondria (arrowheads) 6 hr after CCCP treatment irrespective of genotype. Similar results were obtained 3 hr after CCCP treatment. Scale bar = 10 μm. (d) Model for Parkin translocation and activation. The Parkin Ubl domain masks C-terminal RING-IBR-RING (RBR) domains for E3 activity[46]. A Parkin phosphorylation event at Ser65 (P), combined with unknown factor(s) (?), stimulates the mitochondrial translocation of Parkin, releasing the RBR domains from autoinhibition by the Ubl domain.

the mitochondrial outer membrane proteins. Because inhibition of the degradation of the mitochondrial outer membrane proteins by proteasome inhibitors is reported to block mitophagy[32,35], it may be that the modification of Parkin Ser65 has a greater than expected impact on the mitophagy process. Although our study does not demonstrate that the S65E mutant behaves exactly like the phosphorylated form of Parkin, the S65E mutant does

translocate to the mitochondria in a similar way to WT, although with slightly impaired efficiency, suggesting that S65E has at least some properties that are similar to phosphorylated Parkin. Currently, it is unknown why S65E also inhibits the later processes of mitophagy. One possible explanation is that rapid degradation of phosphorylated Parkin is required for the proper progression of mitophagy, and S65E may not be degraded effectively. However,

there is no evidence that S65E is more stable than WT, as shown in Figure 4c.

Very recently, Kondapalli et al. proposed a model to explain the biological significance of Ser65 phosphorylation, in which Ser65 phosphorylation relieves autoinhibition of Parkin E3 activity by the Ubl domain[18]. This model may explain the depolarised ΔΨm-dependent activation of Parkin. However, our data indicated that the Parkin S65A mutant is also autoubiquitinated (Fig. 4b) and that the ΔUbl mutant showed mild translocation defect and impaired substrate degradation (Supplementary Fig. S8). Moreover, if this is the case, the E3 activity of Parkin pathogenic mutants lacking mitochondrial translocational activity but harbouring intact E3 activity in vitro (such as K161N and K211N, which are subjected to the Ser65 phosphorylation) should be activated in the cytosol[38]. However, our previous data indicate that K161N and K211N are not activated by CCCP treatment[23]. Thus, it is conceivable that another step is required for depolarised ΔΨm-dependent activation of Parkin E3. In addition, the Ubl domain might not only autoinhibit its E3 activity but also contribute to the mitochondrial translocation and the substrate degradation through an as yet unknown mechanism. We believe that an appropriate way to estimate Parkin E3 activity in the context of mitophagy is to evaluate the ubiquitination and degradation of substrates in cells with depolarised ΔΨm. Mfn1 is a well-characterised direct substrate of Parkin[32], and Parkin-dependent poly-ubiquitination modification of Mfn1 can be detected by Western blotting upon ΔΨm depolarisation[32,39,40]. Parkin S65A and S65E appear to ubiquitinate Mfn1, as poly-ubiquitinated forms of Mfn1 were observed (Fig. 4b). However, they cannot degrade it effectively, which suggests that the process of substrate degradation is also impaired in these mutants.

Kondapalli et al. have also shown that T. castaneum PINK1 (TcPINK1) directly phosphorylates human Parkin at Ser65[18]. We confirmed their finding using recombinant TcPINK1 produced from the same construct (Supplementary Fig. S4). The replacement of MBP-Parkin Ser65 with alanine completely abolished PINK1-mediated phosphorylation, indicating that Ser65 is the sole phosphorylation site in vitro. However, experiments in cultured cells showed that the replacement of Ser9, Ser10, Ser101 and Ser198 with alanine affects the Ser65 phosphorylation efficiency (Ser9, ~35% reduction; Ser10, ~76% reduction; Ser101, ~65% reduction; Ser198, ~92% reduction) (Fig. 2a). These residues might be priming phosphorylation sites for Ser65 phosphorylation.

Because PINK1 is believed to be activated in the mitochondria, a topological inconsistency arises from our cell-based data that cytosolic Parkin lacking the mitochondrial translocation activity is phosphorylated. Therefore, it is possible that PINK1 indirectly regulates Parkin phosphorylation. One possible explanation for this is the presence of another cytosolic kinase(s) regulated by PINK1 (Fig. 4d). Alternatively, because mitochondria are a dynamic organelle, cytosolic Parkin adjacent to the moving and fragmented mitochondria with depolarised ΔΨm might be phosphorylated incidentally. The issue as to whether or not PINK1 directly phosphorylates Parkin in cells remains to be solved.

In conclusion, this study has suggested that PINK1-dependent Parkin phosphorylation at Ser65 accelerates the mitochondrial translocation of Parkin and showed that the introduction of mutations at this site also affects subsequent mitophagy processes. Concurrently, our data provide the possibility that there is an elaborate multi-step mechanism for the mitochondrial translocation of Parkin upon the loss of ΔΨm (Fig. 4d), the clarification of which awaits further study.

Methods

Antibodies, plasmids and cell lines. Antibodies used in Western blot analysis were as follows: anti-Parkin (1 : 1,000 and 1 : 5,000 dilution for endogenous and exogenous Parkin, respectively; Cell Signaling Technology, clone PRK8), anti-PINK1 (1 : 1,000 dilution; Novus, BC100-494 or 1 : 1,000 dilution; Cell Signaling Technology, clone D8G3), anti-Mfn1 (1 : 1,000 dilution; Abnova, clone 3C9), anti-VDAC1 (1 : 1,000

dilution; Abcam, Ab15895), anti-Tom20 (1 : 500 dilution; Santa Cruz Biotechnology, FL-145), anti-FLAG-HRP (1 : 2,000 dilution; Sigma-Aldrich, clone M2), anti-GFP (1 : 5,000 dilution; Abcam, ab290), anti-Actin (1 : 10,000 dilution; Millipore, MAb1501), anti-LDH (1 : 1,000 dilution; Abcam, ab7639-1), anti-phospho-GSK3ß (1 : 1,000 dilution; Cell Signaling Technology, clone 5B3), anti-GSK3ß (1 : 1,000 dilution; Cell Signaling Technology, clone 27C10), and anti-Hsp60 (1 : 10,000 dilution; BD Biosciences, clone 24/Hsp60). Antibodies used in immunocytochemistry were as follows: FITC-conjugated anti-GFP (1 : 1,000 dilution; Abcam, ab6662), anti-Tom20 (1 : 1,000 dilution; Santa Cruz Biotechnology, FL-145), anti-Myc (1 : 500 dilution; Millipore, clone 4A6), anti-p62 (1: 500 dilution; Progen Biotechnik, GP62-C), anti-Parkin (1 : 1,000 dilution; Cell Signaling Technology, clone PRK8) and anti-proteasome α7 (1 : 250; a kind gift of Dr S. Murata at the University of Tokyo). cDNAs for human Parkin, PINK1 and its pathogenic and engineered mutants are as described in previous studies[23,41]. Parkin phospho-mutants were generated by PCR-based mutagenesis followed by sequencing confirmation of the entire gene. PINK1⁻/⁻ MEFs, cultured as previously described[23], were retrovirally transfected with pMXs-puro harbouring non-tagged PINK1, PINK1-FLAG, non-tagged Parkin, HA-Parkin, GFP-Parkin and related cDNA; transfected cells were then selected with 1 μg/ml puromycin. HeLa cells maintained at 37°C in a 5% CO₂ atmosphere in Dulbecco's Modified Eagle's Medium (DMEM) supplemented with 10% FCS and 1x non-essential amino acids (GIBCO) were retrovirally transfected with pMXs-puro harbouring non-tagged Parkin along with pcDNA3Hyg-mSlc7a1-VSVG and pcDNA3Hyg-mSlc7a1-FLAG (a kind gift of Dr N. Fujita at UCSD). Stable cell lines were selected with 1 μg/ml puromycin and cloned. Transient transfections of cultured cells were performed using Lipofectamine 2000 (Invitrogen) for plasmids and Lipofectamine RNAiMAX (Invitrogen) for stealth siRNA duplexes (Invitrogen), which were used according to the manufacturer's instructions.

Tissue culture. Skin biopsies were obtained from a PARK6 case and a control without mutations in any known PD genes. The study was approved by the ethics committee of Juntendo University, and all participants gave written, informed consent. Dermal primary fibroblasts established from biopsies were cultured in high glucose DMEM supplemented with 10% foetal bovine serum, 1x non-essential amino acids, 1 mM sodium pyruvate (GIBCO), 100 μM 2-mercaptoethanol, and 1% penicillin–streptomycin at 37°C in a 5% CO₂ atmosphere.

Mapping of Parkin phosphorylation sites. PINK1⁻/⁻ MEFs (6.0 x 10⁷) expressing HA-Parkin and PINK1-FLAG were treated with or without 30 μM CCCP for 30 min. HA-Parkin (~500 ng in each) immunopurified with anti-HA-conjugated agarose beads was eluted with 8 M urea buffered with 50 mM Tris-HCl at pH 9.0. Samples from two independent experiments were digested with trypsin or chymotrypsin and analysed by nano-scale liquid chromatography-tandem mass spectrometry (Dionex Ultimate3000 RSLCnano and ABSciex TripleTOF 5600) followed by MASCOT searching and Mass Navigator/PhosPepAnalyzer processing for identification and label-free quantitation, respectively[42]. Determination of phosphosite localisation was performed based on the presence of site-determining ions[43].

Phosphorylation assay and mitochondrial fractionation. PINK1⁻/⁻ MEFs harbouring HA-Parkin along with wild-type or a kinase-dead form of PINK1-FLAG were metabolically labelled with 175 μCi/ml of [³²P] orthophosphate in phosphate-free DMEM (GIBCO) with 10% FBS at 37°C for 3 hr. The medium was then replaced with fresh DMEM containing 10% FBS. Cells were treated with CCCP for 1.5 hr and were lysed on ice with lysis buffer containing 0.2% NP-40, 50 mM Tris (pH 7.4), 150 mM NaCl and 10% glycerol supplemented with protease inhibitor (Roche Diagnostics) and phosphatase inhibitor (Pierce) cocktails, and HA-Parkin and PINK1-FLAG were immunoprecipitated with anti-HA (Wako Pure Chemical, clone 4B2)- or anti-FLAG (Sigma-Aldrich, clone M2)-conjugated agarose beads. Immunoprecipitates were separated by SDS-PAGE and transferred onto a PVDF membrane. Autoradiography and Western blotting were performed to visualise proteins. Phos-tag Western blotting was performed as previously described[28]. Briefly, phospho-Parkin and phospho-PINK1 were separated on 8% gels containing 50 μM Phos-tag. Mitochondrial and cytosolic fractionations were performed as previously described, with some modifications[20]. The cytosolic fractions were further clarified by a second centrifugation at 105,000 g for 60 min to remove residual organelle membranes.

Immunocytochemical analysis. Cells plated on 3.5 mm glass-bottom dishes (MatTek) were fixed with 4% paraformaldehyde in PBS and permeabilised with 50 μg/ml digitonin for anti-Tom20 and anti-p62 staining or with 0.1% NP-40 for anti-α7 staining in PBS. Cells were stained with anti-Tom20 or anti-α7 antibodies in combination with FITC-conjugated anti-GFP antibody and were counterstained with DAPI for nuclei. Cells were imaged using laser-scanning microscope systems (TCS-SP5, Leica or LSM510 META, Carl Zeiss).

Statistical analysis. A one-way repeated measures ANOVA was used to determine significant differences between multiple groups unless otherwise indicated. If a significant result was achieved ($p < 0.05$), the means of the control and the specific test group were analysed using the Tukey-Kramer test.

1. Valente, E. M. et al. Hereditary early-onset Parkinson's disease caused by mutations in PINK1. Science **304**, 1158–1160 (2004).

2. Takatori, S., Ito, G. & Iwatsubo, T. Cytoplasmic localization and proteasomal degradation of N-terminally cleaved form of PINK1. *Neurosci Lett* **430**, 13–17 (2008).
3. Beilina, A. *et al.* Mutations in PTEN-induced putative kinase 1 associated with recessive parkinsonism have differential effects on protein stability. *Proc Natl Acad Sci U S A* **102**, 5703–5708 (2005).
4. Silvestri, L. *et al.* Mitochondrial import and enzymatic activity of PINK1 mutants associated to recessive parkinsonism. *Hum Mol Genet* **14**, 3477–3492 (2005).
5. Sim, C. H. *et al.* C-terminal truncation and Parkinson's disease-associated mutations down-regulate the protein serine/threonine kinase activity of PTEN-induced kinase-1. *Hum Mol Genet* **15**, 3251–3262 (2006).
6. Clark, I. E. *et al.* Drosophila pink1 is required for mitochondrial function and interacts genetically with parkin. *Nature* **441**, 1162–1166 (2006).
7. Park, J. *et al.* Mitochondrial dysfunction in Drosophila PINK1 mutants is complemented by parkin. *Nature* **441**, 1157–1161 (2006).
8. Yang, Y. *et al.* Mitochondrial pathology and muscle and dopaminergic neuron degeneration caused by inactivation of Drosophila Pink1 is rescued by Parkin. *Proc Natl Acad Sci U S A* **103**, 10793–10798 (2006).
9. Kitada, T. *et al.* Mutations in the parkin gene cause autosomal recessive juvenile parkinsonism. *Nature* **392**, 605–608 (1998).
10. Imai, Y., Soda, M. & Takahashi, R. Parkin suppresses unfolded protein stress-induced cell death through its E3 ubiquitin-protein ligase activity. *J Biol Chem* **275**, 35661–35664 (2000).
11. Shimura, H. *et al.* Familial Parkinson disease gene product, parkin, is a ubiquitin-protein ligase. *Nat Genet* **25**, 302–305 (2000).
12. Zhang, Y. *et al.* Parkin functions as an E2-dependent ubiquitin- protein ligase and promotes the degradation of the synaptic vesicle-associated protein, CDCrel-1. *Proc Natl Acad Sci U S A* **97**, 13354–13359 (2000).
13. Deas, E. *et al.* PINK1 cleavage at position A103 by the mitochondrial protease PARL. *Hum Mol Genet* **20**, 867–879 (2011).
14. Jin, S. M. *et al.* Mitochondrial membrane potential regulates PINK1 import and proteolytic destabilization by PARL. *J Cell Biol* **191**, 933–942 (2010).
15. Meissner, C., Lorenz, H., Weihofen, A., Selkoe, D. J. & Lemberg, M. K. The mitochondrial intramembrane protease PARL cleaves human Pink1 to regulate Pink1 trafficking. *J Neurochem* **117**, 856–867 (2011).
16. Whitworth, A. J. *et al.* Rhomboid-7 and HtrA2/Omi act in a common pathway with the Parkinson's disease factors Pink1 and Parkin. *Dis Model Mech* **1**, 168–174; discussion 173 (2008).
17. Narendra, D. P. *et al.* PINK1 is selectively stabilized on impaired mitochondria to activate Parkin. *PLoS Biol* **8**, e1000298 (2010).
18. Kondapalli, C. *et al.* PINK1 is activated by mitochondrial membrane potential depolarization and stimulates Parkin E3 ligase activity by phosphorylating Serine 65. *Open Biol* **2**, 120080 (2012).
19. Okatsu, K. *et al.* PINK1 autophosphorylation upon membrane potential dissipation is essential for Parkin recruitment to damaged mitochondria. *Nat Commun* **3**, 1016 (2012).
20. Lazarou, M., Jin, S. M., Kane, L. A. & Youle, R. J. Role of PINK1 binding to the TOM complex and alternate intracellular membranes in recruitment and activation of the E3 ligase Parkin. *Dev Cell* **22**, 320–333 (2012).
21. Vives-Bauza, C. *et al.* PINK1-dependent recruitment of Parkin to mitochondria in mitophagy. *Proc Natl Acad Sci U S A* **107**, 378–383 (2010).
22. Geisler, S. *et al.* PINK1/Parkin-mediated mitophagy is dependent on VDAC1 and p62/SQSTM1. *Nat Cell Biol* **12**, 119–131 (2010).
23. Matsuda, N. *et al.* PINK1 stabilized by mitochondrial depolarization recruits Parkin to damaged mitochondria and activates latent Parkin for mitophagy. *J Cell Biol* **189**, 211–221 (2010).
24. Kawajiri, S. *et al.* PINK1 is recruited to mitochondria with parkin and associates with LC3 in mitophagy. *FEBS Lett* **584**, 1073–1079 (2010).
25. Ziviani, E., Tao, R. N. & Whitworth, A. J. Drosophila parkin requires PINK1 for mitochondrial translocation and ubiquitinates mitofusin. *Proc Natl Acad Sci U S A* **107**, 5018–5023 (2010).
26. Sha, D., Chin, L. S. & Li, L. Phosphorylation of parkin by Parkinson disease-linked kinase PINK1 activates parkin E3 ligase function and NF-kappaB signaling. *Hum Mol Genet* **19**, 352–363 (2010).
27. Kim, Y. *et al.* PINK1 controls mitochondrial localization of Parkin through direct phosphorylation. *Biochem Biophys Res Commun* **377**, 975–980 (2008).
28. Imai, Y. *et al.* The loss of PGAM5 suppresses the mitochondrial degeneration caused by inactivation of PINK1 in Drosophila. *PLoS Genet* **6**, e1001229 (2010).
29. Woodroof, H. I. *et al.* Discovery of catalytically active orthologues of the Parkinson's disease kinase PINK1: analysis of substrate specificity and impact of mutations. *Open Biol* **1**, 110012 (2011).
30. Yamamoto, A. *et al.* Parkin phosphorylation and modulation of its E3 ubiquitin ligase activity. *J Biol Chem* **280**, 3390–3399 (2005).
31. Narendra, D., Tanaka, A., Suen, D. F. & Youle, R. J. Parkin is recruited selectively to impaired mitochondria and promotes their autophagy. *J Cell Biol* **183**, 795–803 (2008).
32. Tanaka, A. *et al.* Proteasome and p97 mediate mitophagy and degradation of mitofusins induced by Parkin. *J Cell Biol* **191**, 1367–1380 (2010).
33. Okatsu, K. *et al.* p62/SQSTM1 cooperates with Parkin for perinuclear clustering of depolarized mitochondria. *Genes Cells* **15**, 887–900 (2010).
34. Narendra, D., Kane, L. A., Hauser, D. N., Fearnley, I. M. & Youle, R. J. p62/SQSTM1 is required for Parkin-induced mitochondrial clustering but not mitophagy; VDAC1 is dispensable for both. *Autophagy* **6**, 1090–1106 (2010).
35. Chan, N. C. *et al.* Broad activation of the ubiquitin-proteasome system by Parkin is critical for mitophagy. *Hum Mol Genet* **20**, 1726–1737 (2011).
36. Wang, X. *et al.* PINK1 and Parkin Target Miro for Phosphorylation and Degradation to Arrest Mitochondrial Motility. *Cell* **147**, 893–906 (2011).
37. Liu, S. *et al.* Parkinson's disease-associated kinase PINK1 regulates Miro protein level and axonal transport of mitochondria. *PLoS Genet* **8**, e1002537 (2012).
38. Matsuda, N. *et al.* Diverse effects of pathogenic mutations of Parkin that catalyze multiple monoubiquitylation in vitro. *J Biol Chem* **281**, 3204–3209 (2006).
39. Gegg, M. E. *et al.* Mitofusin 1 and mitofusin 2 are ubiquitinated in a PINK1/parkin-dependent manner upon induction of mitophagy. *Hum Mol Genet* **19**, 4861–4870 (2010).
40. Rakovic, A. *et al.* Mutations in PINK1 and Parkin impair ubiquitination of Mitofusins in human fibroblasts. *PLoS One* **6**, e16746 (2011).
41. Shiba, K. *et al.* Parkin stabilizes PINK1 through direct interaction. *Biochem Biophys Res Commun* **383**, 331–335 (2009).
42. Iwasaki, M., Sugiyama, N., Tanaka, N. & Ishihama, Y. Human proteome analysis by using reversed phase monolithic silica capillary columns with enhanced sensitivity. *J Chromatogr A* **1228**, 292–297 (2012).
43. Beausoleil, S. A., Villen, J., Gerber, S. A., Rush, J. & Gygi, S. P. A probability-based approach for high-throughput protein phosphorylation analysis and site localization. *Nat Biotechnol* **24**, 1285–1292 (2006).
44. Li, Y. *et al.* Clinicogenetic study of PINK1 mutations in autosomal recessive early-onset parkinsonism. *Neurology* **64**, 1955–1957 (2005).
45. Zhou, C. *et al.* The kinase domain of mitochondrial PINK1 faces the cytoplasm. *Proc Natl Acad Sci U S A* **105**, 12022–12027 (2008).
46. Chaugule, V. K. *et al.* Autoregulation of Parkin activity through its ubiquitin-like domain. *EMBO J* **30**, 2853–2867 (2011).

Acknowledgements

Author contributions

K.S., Y. Imai and N.H. designed the research; K.S., Y. Imai, S.Y., T.K. and Y. Ishihama performed the experiments; S.S. contributed new reagents/analytic tools; K.S. and Y. Imai analysed the data; and Y. Imai and N.H. wrote the paper. K.S. and Y. Imai contributed equally to this work.

Additional information

How to cite this article: Shiba-Fukushima, K. *et al.* PINK1-mediated phosphorylation of the Parkin ubiquitin-like domain primes mitochondrial translocation of Parkin and regulates mitophagy. *Sci. Rep.* **2**, 1002; DOI:10.1038/srep01002 (2012).

Q05 パーキンソン病の発症に遺伝子の関与はあるのか？

結論から先に

◉ 遺伝子の関与は大きい！

◉ パーキンソン病は，約5〜10％に家族性パーキンソン病を認め，パーキンソン病の発症に遺伝子が少なからず関与していると考えられる。

◉ これまでの解析で，単一遺伝子異常がパーキンソン病の5〜30％以上で同定されてきている。ただし人種により頻度に差がある。

◉ また，孤発性パーキンソン病では10〜20％以上に発症の危険因子や保護的因子として働く遺伝的因子が明らかにされている。

◉ パーキンソン病は，"単一遺伝子異常により，または多くの遺伝的因子を背景とし加齢因子，環境因子との相互作用により発症する多因子遺伝性疾患"と考えられてきている。

◉ 遺伝子，遺伝的因子の関与は少なく見積もってもパーキンソン病の20〜30％で示唆され，今後ここ数年のうちにも次世代シークエンサーを用いた網羅的な遺伝子解析により，さらに多くの知見が蓄積されていくものと思われる。

① パーキンソン病はどれくらいありふれた疾患か？ その病態・原因は？

☐→ パーキンソン病はアルツハイマー病についで2番目に多い神経変性疾患で，有病率は10万人に125人（1,000人に1人，0.1％）と考えられ，加齢を危険因子として65歳以上では約2％（50人に1人）がパーキンソン病に罹患するとの報告もあり，頻度の高い疾患といえます。今後高齢化社会が進むにつれ，ますます患者が増えていくものと考えられます。

☐→ パーキンソン病の大部分は孤発型ですが，約5〜10％に家族性パーキンソン病を認め，パーキンソン病の発症に遺伝的因子が少なからず関与していると考えられます。

☐→ これまでのところパーキンソン病の根本の原因については不明ですが，黒質神経細胞が脱落し，1つの遺伝子異常により，または複数の遺伝的因子と加齢因子と環境因子との相互作用，組み合わせにより閾値を超えると発症する多因子疾患である，という考え方が主流となってきています。